The Ozarks Environmental and Water Resources Institute (OEWRI)
Missouri State University (MSU)

Big River Mining Sediment Assessment Project

DC-Resistivity and Ground Penetrating Radar Investigation of the Floodplain and Gravel Bars of the Big River, Eastern Missouri

Prepared by:

Kevin L. Mickus, Ph.D., Co-Principal Investigator
Robert T. Pavlowsky, Ph.D., Principal Investigator
Marc R. Owen, M.S., Research Specialist II
Patrick J. Womble, M.S., Research Assistant

Ozarks Environmental and Water Resources Institute
Missouri State University
901 South National Avenue
Springfield, MO 65897
bobpavlowsky@missouristate.edu

Funded by:
U.S. Fish and Wildlife Service
Cooperative Ecosystems Studies Unit

David E. Mosby, Environmental Contaminants Specialist
Columbia Missouri Field Office
573-234-2132 Ext. 113
Dave_Mosby@fws.gov

June 18, 2010

TABLE OF CONTENTS

LIST OF TABLES

LIST OF FIGURES

ABSTRACT

A DC-resistivity (DCR) and ground penetrating radar (GPR) study was conducted on the floodplains and gravel bars at four sites along the Big River in eastern Missouri to determine if DCR and GPR measurements can be used to determine the sedimentological characteristics of the floodplains and gravel bars, thickness of the floodplain deposits and if these methods could determine the extent of contaminated sediments. GPR data were collected at 100 and 250 MHz along profiles perpendicular and parallel to the river to image sedimentary structures of different scale lengths. DCR measurements were collected on the floodplains using a Schlumberger array along the same profiles as the GPR profiles. Constrained by sediment cores along most of the profiles, GPR data were best at imaging the bottom of a silt-loam layer that occurred between 2 and 2.5 meters below the surface. The DCR measurements provided the most constraints on the nature of the floodplain deposits. DCR was able to image the thickness of the sediments at all sites except at St. Francois State Park. The floodplain core determined depth of 8.5 meters was beyond the depth that could be imaged with the system used. A more powerful system could easily image at this depth, so there was a limitation factor of the system used. Two-dimensional DCR models indicated that the resistivity of the floodplain sediments decreases downstream. At Morse Mill, Cedar Hill and Washington State Park, the floodplain sediments had electrical resistivities less than 50 ohm-m with thicknesses between 4 and 6 meters. St. Francois State Park was an exception with two areas of higher surface resistivities (~110 ohm-m) that were 2 meters thick and another area with thick (at least 8 meters) of higher electrical resistive material. These higher electrical resistivities may be indicative of more coarse grain material in an old channel fill deposit. The GPR and DCR methods used in this study could not delineate between the contaminated and uncontaminated sediments.

INTRODUCTION

The Old Lead Belt is a historic lead (Pb) and zinc (Zn) mining sub-district within the Southeast Missouri Lead Mining District which was a leading producer of Pb worldwide from 1869 to 1972. During the century-long mining period, large volumes of metaliferous wastes were produced during ore processing and stored at dump sites near the mill. Studies have shown that at least some of this waste material has moved into the nearby Big River where fluvial processes can disperse contaminated mining sediments far downstream (Schmitt and Finger, 1982; James 1989, 1991; Knighton, 1989; Smith and Schumacher, 1993; Roberts et al., 2009). In the Big River, the transport of mining sediment has potential ecological implications on a number of endangered species living in the lower valley near the confluence with the Meramec River. As used here, mill tailings-derived materials released to the river that are transported and deposited downstream are generally referred to as mining sediment. Mining sediment is a mixture of

natural watershed-derived materials and varying amounts of lead (Pb) and zinc (Zn) present in mill wastes, chat, or tailings that have been released to nearby water bodies from original on-site dump areas near the mine by geomorphic or human processes. Mining sediments contain high levels of Pb and Zn in concentrations that are known to exceed probable effects concentrations of 128 ppm in sediments within the channel and 459 ppm in floodplain sediments (MacDonald et al. 2000; MDNR, 2007a; Roberts et al., 2009).

Currently, geomorphological and geochemical studies are being used to investigate the amount of lead in floodplain and gravel bar deposits within the current channel environment using a variety of discrete sediment sampling techniques. Coring floodplain and bar features, for instance, can provide detailed information on these deposits, however, it is expensive and only provides information at one location. Furthermore, these methods cannot determine the overall startigraphy or geometry of the entire floodplain or bar features without a great deal of uncertainty when extrapolating data points between samples locations. To aid in the determination of the composition and volume of these features, geophysical methods have been used to evaluate the stratigraphy of river deposits, including floodplains (Jol and Smith 1991; Asprion and Aigner 1997; Neal 2004; Engels and Roberts 2005; Kostic and Aigner, 2007; LeClerc and Hickin, 2009).

To obtain a spatially significant picture of the subsurface stratigraphy, a variety of geophysical methods (e.g., seismic, DC-resistivity (DCR), electromagnetics (EM), ground-penetrating radar (GPR)) can be used. Methods such as DCR, EM and GPR are commonly used for river sediment studies because the contrast in electrical conductivity and the dielectric contrast between various sediments are usually of a larger magnitude than the contrast in other physical properties (e.g., seismic velocity, density) (Reynolds, 1997).

The purpose of this study is to assess the applicability of using combined DCR and GPR measurements in order to determine the geometry, composition, and contamination levels of floodplain and gravel bar deposits in the Big River. The objectives of this study are; (1) use combined DCR and GPR measurements along with soil core data to determine the depth and contamination level of floodplain deposits, (2) use GPR measurements and tile probe information on gravel bar deposits to determine the depth and contamination level of the deposit, and (3) assess the overall applicability of these methods in this geomorphologic setting.

STUDY AREA

Geology and Soils

The Old Lead Belt and Big River are primarily located on the Salem Plateau of the Ozarks Highlands. The Big River drains about 2,500 km^2 before it flows into the Meramec River near Eureka, Missouri. Land elevations range from 700 to 1,000 ft above sea level. The rugged terrain is well-dissected with narrow divides. The headwaters of the river are in the St. Francois Mountains which are composed of igneous rocks (MDNR, 1979). However, most of the drainage area of the Big River is underlain by dolomite with some limestone and shale units. Sandstones outcrop locally in the southern and northern portions of the basin. The chief host-rock of Pb and Zn mineralization is the Cambrian-age Bonne Terre Dolomite of which outcrops at the surface in the southern and eastern portions of the basin. The main ore minerals are galena (Pb-sulfide), sphalerite (Zn-sulfide), and some smithsonite (Zn-carbonate). Other sulfides found in association with Pb-sulfide include pyrite (Fe-sulfide, gangue) and various copper sulfides (Smith and Schumacher, 1993). The richest deposits are found in association with shale layers and breccias in the lower third of the formation. In the area, the Bonne Terre Dolomite is typically from 375 to 400 ft thick and typically 200 to 1000 ft deep, but it is exposed at the surface in some places. Upland soils in the area are typically formed in a thin layer of silty Pleistocene loess overlying cherty or non-cherty residuum formed in dolomite, limestone, and shale (Brown, 1981).

Mining History

The Old Lead Belt Mining Sub-district is located in St. Francois County, about 110 km south of St. Louis (Figure 1). Lead was first mined in the region between 1742 and 1762. Up until the middle 1800s, mining involved the extraction of relatively large galena crystals from shallow pits. Around 1864, the first organized mining operations began in Bonne Terre and large-scale mining began in the Old Lead Belt around 1904. Gravity milling produced coarse chat wastes until the 1930s, after which it was phased out following the introduction of froth flotation in 1917, which was more productive but produced a large amount of fine-grained tailings. Annual metallic lead production peaked in 1942 and the last mine closed in 1972. About 227 million Mg of tailings were produced during the mining period with coarse chat wastes stored in large piles. Fine tailings were slurried and transported by pipe to impoundments, called slime ponds, into dammed valleys (Newfield, 2006).

METHODS

Data Collection Locations

Geophysical data collection involved both DCR and GPR measurements along floodplains and GPR measurements on gravel bars at four sites along the Big River downstream of the old mining district. The four sites, from upstream to downstream, are: St. Francois State Park, Washington State Park, Morse Mill Park, and Cedar Hill Park. The location of each site and the number of DCR and GPR profiles used in this study are given here:

1. **St. Francois State Park** is located at river km 141 in St. Francois County and is the site closest to the former mill and tailings pile sites. Three GPR and DCR profiles were collected on the floodplain and 2 GPR profiles were collected on the gravel bar (Figure 2). Line 1 was collected perpendicular to the main channel and lines 2 and 3 were recorded parallel to the main channel approximately 30 m apart. Line 4 was collected on the gravel bar perpendicular to the main channel, while line 5 was collected parallel to the main channel.

2. **Washington State Park** is located at river km 101.7 in Jefferson County near the confluence with Mineral Fork. One GPR and DCR profile were collected on the floodplain at Washington State Park perpendicular to the main channel (Figure 3). Gravel bar data was not collected at Washington State Park due to high water levels.

3. **Morse Mill Park** is located in Jefferson County at river km 49.8 upstream of an old mill dam. Three GPR profiles and DCR profiles were collected on the floodplain and 2 GPR profiles were collected on the gravel bar (Figure 4). Line 1 was collected perpendicular to the main channel and lines 2 and 3 were parallel to the main channel on the floodplain about 65 m apart. Line 4 was collected on the gravel bar parallel to the main channel, while line 5 was collected perpendicular to the main channel.

4. **Cedar Hill Park** is also the site of a former mill dam located in Jefferson County at river km 32.7. Three DCR and GPR profiles were collected on the floodplain at Cedar Hill. Line 2 is approximately 40 meters west of line 1 and both are perpendicular to the main channel. Line 3 is also perpendicular to the main channel, but located on the gravel bar.

Characterization of Alluvial Deposits

Floodplain Cores

Overbank sediment samples were collected with a truck-mounted Giddings coring rig along across-valley transects to check for vertical and lateral variations in contaminated layer thickness. Field descriptions of each core included color, texture, structure, and the presence of artifacts. The targeted deposits contain evidence of little to no soil development indicating that they are relatively young and formed during the historical mining period. An attempt was made to sample at least two different floodplain units at each reach: high floodplain (older) and low floodplain (younger) deposits as determined in the field or located on soil maps (Brown, 1981).

Bar Sampling

Channel bars are depositional features that are exposed above the water line during low flow conditions. Bar sediment samples were collected by shovel at a depth of approximately three times the maximum clast size observed on the bar surface in order to exclude the influence of surface armoring on sediment measurements (Rosgen, 1996). Typically, three samples were collected down the centerline of each bar at the head, middle, and tail locations. Where possible, at least two different bar deposits were sampled within each reach. Samples were stored in labeled 1-quart plastic freezer bags. To estimate the thickness of the chat-sized sediment and scour depth in the channel, refusal depths in the bed and bar areas were determined with a tile probe at 5 to 10 locations across the active channel.

Geochemical analysis

Floodplain and bar samples were measured by X-ray Fluorescence (XRF) analysis used in the field and OEWRI laboratory to determine the geochemistry of mining and background sediment samples. Several other studies have also used similar analytical technology to determine levels of sediment contaminants in the Big River (MDNR, 2001, 2003, 2007a; Roberts et al. 2009). In the present study, an Oxford Instruments X-MET 3000 TXS+ was used to determine the concentrations of Pb, Zn, Fe, Mn, and Ca in tailings, channel, floodplain, and control site sediment samples in <2mm fraction.

Grain-size Distribution

Bar samples were hand sieved to determine particle size distribution and isolate size fractions for further analysis. Specific size fractions are reported as a percentage of total mass of the bulk sample passing through a 64 mm sieve. Larger clasts (>64 mm) were excluded from sampling because they were too large for the sampling procedures being used, represent a relatively small fraction of the glide, bar, and bank deposits sampled for this study, and rarely originate from mining sources. Sieving was conducted manually on dry samples.

Geophysical Data Collection and Processing

DC-Resistivity

DCR measurements were acquired with a MiniRes four-electrode system using the Schlumberger electrode array configuration. At all stations, the potential electrode distance was 1 meter and distance from the potential to current electrode was varied between 3 and 21 meters. The distance between individual Schlumberger soundings was 3 meters. Profiles were acquired at all sites perpendicular and parallel to the Big River on the floodplain except at Washington State Park where only a profile perpendicular to the river was acquired (Figs. 1-4)

To quantitatively interpret the DCR results, data along each profile were inverted individually using a two-dimensional inversion routine that inverts for the subsurface resistivity structure (Loke and Barker 1996). A robust-constrained (l_1 norm) that included topography was used in the inversion process along each profile. Since inversion of geophysical data is nonunique, data used in this study were inverted along each profile by varying the starting model, data weights, smoothness factor and damping factor in order to determine which resistivity structures were required by the data.

Ground Penetrating Radar

GPR is an electromagnetic prospecting device where an electromagnetic pulse (or wave) is transmitted through the subsurface with a portion of the pulse reflected at boundaries caused by changes in the electromagnetic properties within the subsurface. Typically, a pulse is transmitted using antennae with frequencies ranging from 25 MHz to 1000 MHz, where lower frequencies penetrate deeper into the subsurface than higher frequencies (e.g., 30 m for 25 MHz and 2 m for 200 MHz (Annan 1992)). However, higher frequencies will provide higher spatial resolution. Given this tradeoff between depth penetration and resolution, it is advantageous to use two or more different antennas in order to obtain the maximum amount of subsurface information.

A Mala Ramac GPR system with a centered frequency and shielded antenna at frequencies of 100 and 250 MHz in a monostatic mode was used to collect the data. At each of the four sites, at least one profile was collected perpendicular and parallel to the river channel using both antennae. The use of multiple antennae provide more subsurface information of a region. However, due to the 100 MHz antenna breaking at Morse Mill, only 250 MHz data were collected at Washington and St. Francois State Parks.

Data from each profile were processed separately. Since GPR data are similar to seismic reflection data, the methods used to process seismic reflection data are commonly used on GPR data (Conyers 2004, 2006). However not all processing techniques are used since small-scale, high amplitude reflections and diffractions are used in GPR to locate small-scale features that are

common in archaeological surveys (Conyers 2004). Therefore, time migration methods that move diffraction patterns and dipping reflectors to their true locations are not commonly used.

The most commonly used processing technique is the removal of background noise which is commonly caused by ringing of the antennae. This causes high amplitude horizontal bands that often obscure any reflections of interest. To compensate for this, background removal function was applied to all of the profiles. Amplitudes of the reflections recorded at the same time were summed and then divided by the number of traces added together. The resultant trace is then subtracted from the original data set (Conyers, 2004). Additionally, automatic gain control and spherical divergence corrections were applied to account for amplitude loses with depth due to the absorption and loss of the energy with depth. High frequency noise was suppressed by applying low-pass filter with cutoff frequencies ranging from 1200 to 2200 MHz depending on the profile.

The last processing technique was predictive deconvolution. Predictive deconvolution is performed in order to suppress multiples and to compress the source wavelet in order to better define prominent reflectors on the profile. This technique is not commonly applied to GPR data as it may suppress subtle reflections that may be due to small features (Conyers 2004). However, the authors performed predictive deconvolution on some of the profiles because most profiles were affected by multiples.

RESULTS AND DISCUSSION

Site Characteristics and Stratigraphy

St. Francois State Park

The valley floor, defined here as the extent of mapped alluvial soils, at this site is narrow (0.1 km) and the river is confined by a bluff along the left bank (Table 1; Brown, 1981). On the opposite bank from the bluff an extensive gravel bar has formed around 20 m wide, 150 m long and about 2.5 m deep (Table 2). The sediment composition of the bar is about 49% fine-grain material (<2 mm) and 9% coarse gravel (>16 mm). The mean Pb concentration found in the fine-grain fraction within the bar is 1,027 ppm. Two floodplain surfaces within this reach were identified with the near channel surface being about 0.5 m below the upper floodplain surface (Figure 6). The floodplain here consists of brown silt-loam, over sand and small gravel, over coarse gravel lag. Thickness of the silt-loam deposit is 3.9 m on the near channel surface and 4.5 m on the upper floodplain surface. Thickness of the sand and small gravel deposit is 3.7 m in the near channel surface and 3.1 m on the upper floodplain surface. Floodplain contamination with Pb concentrations >400 ppm are 6 m deep in the near channel surface and 1.5 m deep on the

upper floodplain surface. The mean Pb concentration within the contaminated floodplain sediment is 1,673 ppm in the near channel and 2,837 ppm on the upper floodplain surface. Peak Pb concentration, the highest Pb concentration in the core, is 3.8 m deep (5,542 ppm) in the near channel floodplain and 1.1 m deep (7,287 ppm) in the upper floodplain.

Washington State Park

The valley bottom at this site is 0.6 km wide as the river is becoming more sinuous within the valley where a significant floodplain and bar is being built along the left bank. The channel is also migrating into an low terrace deposit on the opposite bank exposing a 10 m cutbank of older alluvium. There are three distinct areas within the floodplain at this site; a near channel floodplain, upper floodplain, and backswamp. The highest point of the upper floodplain surface is about 2 m above the middle of near channel surface before it grades down about 1 m to the backswamp against the valley wall (Figure 7). The floodplain is also a brown silt-loam 4 m deep over a sand/gravel layer that is around 3.4 m deep that overlies a coarse gravel lag. The near channel surface has around 4 m of brown silt-loam over 2 meters of sand/gravel over coarse gravel lag. The backswamp location has 2.8 m of brown silt-loam over 2.1 m of sand/gravel over coarse gravel lag. Contamination with Pb concentrations >400 ppm are 3.6 m deep in the near channel surface, 2.1 m deep on the upper floodplain surface, and 0.7 m deep in the backswamp. Mean Pb concentrations within the contaminated sediment zone is 1,206 ppm in the near channel deposit, 1,644 ppm on the floodplain, and 832 ppm in the backswamp. The peak Pb concentration is 1.4 m deep (2,220 ppm) on the near channel floodplain, 1 m deep (12,307ppm) on the upper floodplain, and 0.7 m deep (4,426 ppm) in the backswamp.

Morse Mill Park

The valley here is 0.9 km wide as the river meanders here are much larger with multiple terrace surfaces being abandoned on both sides of the river. A small gravel bar deposit exists along the right bank above the dam that is 17 m wide, 88 m long and about 2 m deep. The sediment composition of the bar is about 32% fine-grain material (<2 mm) and 18% gravel (>16 mm). The mean Pb concentration found in the fine fraction within the bar is 237 ppm. A near channel floodplain surface is about 0.6 meters below the upper floodplain surface at this location (Figure 8). The near channel floodplain here consists of 3.6 m of brown silt-loam over sand/gravel deposits. The upper floodplain has 2.4 m of brown silt-loam over sand and small gravel. Depth to coarse gravel lag is unknown. Floodplain contamination of Pb concentrations >400 ppm are 2.6 m deep in the near channel surface and only 1.2 m deep on the upper floodplain surface. Mean Pb concentrations in the contaminated sediment is 1,581 ppm in the near channel and 682 ppm in the floodplain deposits. The peak Pb concentration found 1 m deep (6,526 ppm) in the near channel floodplain and 0.8 m deep (1,350 ppm) in the upper floodplain.

Cedar Hill Park

The valley here is the widest at 1 km of the four sites in this study. The left bank along this reach is a bedrock outcrop along a strath terrace and the right bank has a well-formed floodplain. There is a greater elevation difference between the two floodplain surfaces at this site compared to the other with the near channel surface about 1.5 meters below the upper floodplain surface (Figure 9). Floodplain contamination with Pb concentrations >400 ppm are 3.6 m deep on the near channel surface and 0.4 m deep on the upper floodplain surface. Mean Pb concentrations in contaminated sediment zones are 1,160 ppm near the channel and 278 ppm in the upper floodplain deposit. The peak Pb concentration is 1.7 m deep (3,229 ppm) in the near channel floodplain and 0.2 m deep (781 ppm) in the upper floodplain.

DCR and GPR Floodplain Analysis

DCR and GPR results can be used to image the electrical conductivity structure beneath the floodplain of the Big River. The GPR method have the advantage of ease and speed of data collection and providing detailed resolution of sedimentary structures while the DCR measurements are useful in defining the overall depths and conductivities of electrical structure but do not have the resolution to determine the location of small-scale sedimentary structures. The disadvantage of the GPR method is that it is sensitive to materials with high dielectric permittivities (e.g., water and clays) and these materials will absorb the signals and limit depth penetration. Comparing the two data sets, one notices that there are several regions with resistivity anomalies that correspond to several possible sedimentary structures (or changes within the reflectors, see arrows) within the floodplain sediments. One example is seen on line 1 at St. Francois State park where the high resistivity seen on the DCR image at 17.3 m is expressed by deeper reflectors on the GPR image (Figures 10 and 11). Below is a description of each of the four sites will be given. At each location, also shown are topographic profiles and the stratigraphy of the floodplain cores if available.

St. Francois State Park

The GPR profile indicates that the floodplain consists of horizontal reflectors that extend to 2.0 meters in depth except around 15 to 22 m where the reflectors are deeper and are dipping (Figure 10). The majority of the reflectors appear to be imaging the base of the silt-loam deposit, which is approximately 2.5 m deep, except possibly between 15 and 22 m. The region between 15 and 22 m corresponds to a higher resistivity region seen on the DCR model (Figure 11). The high resistivity region that occurs near the break between surfaces, which was not cored, may correspond to an old channel fill that is sandy and/or contains a significant amount of gravel. This high resistivity layer extends to the surface to approximately 30 m. The source of this layer is unknown but may be a higher sandy material. Additionally, there is a thin layer (1.0-1.5 m) of higher resistivity layer along the northern section of the model that appears to be more coarse-

grained than the silt-loam deposit. Below the higher resistivity layer along both the northern and southern sections of the profile, the resistivities decrease with lower values in the north. There is no indication of the total depth of the floodplain sediments by the DCR models, but the depth is at least 8.0 m. This is verified by the floodplain cores that hit coarse gravel lag at 7.6-8.6 m along the profile. The depth to coarse gravel lag was only partially determined and using larger current spacing would help in rectifying this problem. The system used would allow a maximum current spacing of 23 m. No distinction between contaminated and uncontaminated deposits can be seen in line 1.

For lines 2 and 3, the GPR profiles show the same horizontal reflectors as seen on line 1 (Figures 12 and 14). Also, as seen on line 1, deeper reflectors can be seen where the DCR models indicate higher resistivities (e.g., east of 24 m on Figure 13 and the western half of Figure 15). The DCR models show the higher resistivity surficial material that was seen on the perpendicular model but it is not continuous across the floodplain. The models indicate that the western portions of the floodplains contain higher resistivity material than the eastern portions of the floodplain. Line 2 does indicate that the floodplain sediments are thinner than the other models and varies between 6.5 and 8.5 m. No distinction between contaminated and uncontaminated deposits can be seen in lines 2 and 3.

Washington State Park

Both the GPR profile and DCR model indicate that the floodplain at Washington State Park does not have significant electrical resistivity features within the floodplain sediments. The GPR profile shows parallel reflectors down to approximately 2.0 meters and may image the bottom of silt-loam material which is approximately 4.0 m (Figure 16). However, the DCR model shows that the depth to the coarse gravel lag varies from north to south (Figure 17). The thickness is approximately 4.0-4.5 m in the north and thickens to 7.0-8.0 m in the south, which follows closely the floodplain core data. Resistivity values are higher here than at St. Francois State Park for the depth to coarse gravel lag, although it is more shallow. Additionally, the lower electrical resistivity values are probably caused by water infiltration near the river at other sites are not seen at Washington State Park. No distinction between contaminated and uncontaminated deposits can be seen in this profile.

Morse Mill

Reflections from line 1 can be seen to about 2.5 m from GPR data collected with the 100 MHz and 250 MHz antenna (Figure 18 and 19). Noteable regions include stronger, deeper reflections around 27 to 36 m on both profiles but more prevalent on the 100 MHz profile. The source of these reflections may be the base of the silt-loam layer. This region can be seen on the DCR model as a higher resistivity region and could be caused by sand deposits that may be an old channel fill (Figure 20). To the south of this high resistivity region, the depth to refusal on the

DCR model is approximately 8.0 m and the maximum depth of reflections deepen as well. At 40 m the reflections dip indicating that the silt-loam deposits are thickening. The other notable resistivity feature is a higher resistivity zone at 58 m that may represent thinner (4.5 m) floodplain sediments. This zone is roughly seen on the 100 MHz at 60 m by a slight northward dipping of the reflections. The DCR model also shows the low resistivity values near the channel that may be caused by saturation of the bank material near the water. No distinction between contaminated and uncontaminated deposits can be seen along line 1.

The 100 MHz GPR antenna broke while collecting profile 2, so only line 1 contains 100 MHz data. Consequently, the other sites only have 250 MHz data available for analysis. Both the GPR profiles and DCR models indicate roughly uniform electrical resistivity structure with depths to refusal varying from 8 meters along DCR profile 2, which is closer to the river, to 6 m further away from the river on DCR profile 3 (Figures 21-24). Additionally, the electrical resistivities decreased farther away from the river, indicating that sediment is fining away from the current channel position. This cannot be verified without more detailed analysis of the grain-size distribution in the floodplain cores. The GPR profiles show horizontal layering except at 29 meters on line 2 where a small scour structure is indicated. Again, no distinction between contaminated and uncontaminated deposits can be seen in lines 2 and 3.

Cedar Hill

For the first 15 m of line 1 the depth to sand is approximately 2.5 m and the depth shallows toward the south for the 100 MHz antenna (Figure 25). Reflections become more discontinuous, which suggest that some type of variation in the sedimentary structures may exist within the floodplain deposits and could indicate that there is a fining of the sediment away from the current channel location. The 250 MHz antenna does not indicate a strong reflector at 2.5 m and this is probably due to the limited depth penetration of this antenna in the fine-grained sediments (Figure 26). However, the profile does indicate the same general pattern of sediment thickening from 0 m to approximately 13 m and there is a lack of definitive reflectors in the southern half of the profile.

The DCR model from line 1 does not image the base of the sand layer, but probably images the total thickness of the floodplain deposits, which is approximately 4.5-5.0 m (Figure 27). This cannot be verified with core data because it did not reach the depth to coarse gravel lag. However, the range of reflectors within the sedimentary structures is similar to Washington State Park where more detailed core data are available. The final model shows that the northern part of the profile has low resistivity values, similar to the Morse Mill models, which is probably due bank saturation near the channel and the likely cause of poor GPR results in this area of the profile. One note, the DCR model is four meters off the GPR profile. The DCR model shows that the upper floodplain sediments are composed of a low resistivity material that is slightly

lower here at 20-25 ohm-m compared to 30-35 ohm-m at Morse Mill. This may reflect grain-size differences between the two sites. The electrical resistivity at Cedar Hill and Morse Mill are significantly lower than at Washington State Park (approximately 50 ohm-m) indicating a fining of the floodplain sediment downstream. The sediments are thickest at 18 m (which agrees with the general trend of the GPR results) and 30 m. No distinction between contaminated and uncontaminated deposits in the GPR or DCR data can be seen along line 1.

The 100 MHz and 250 MHz GPR profile from line 2 suggests that the depth to the bottom of the sand layer is between 2.5 and 3.0 m, however, detailed core data are not available for this profile to confirm this (Figure 28 and 29). The DCR model suggests that the thickness of the floodplain sediments is at least 4.0 m deep or thicker (Figure 30). The northern portion of the DCR model indicates low resistivity values which is probably due to bank saturation. This may be the reason the GPR images do not penetrate below 3.0 m. The GPR images do show a thickening of the sediment toward the river at 5-6 m. In general, the floodplain sediments are thicker in this region than along line 1 and there is no indication of sedimentary structures within the sediments along line 2. No distinction between contaminated and uncontaminated deposits can be seen in lines 2 and 3.

GPR Analysis of Gravel Bars

Stratigraphy

Parallel profiles show the distribution of alluvial structures in the downstream direction whereas perpendicular profiles show the distribution across the channel. Reflections in both profiles parallel to the channel exhibit a wavy pattern along the entire length of the profile (Figure 31 and 32). Wavy patterns result from the accretion of sediment onto the downstream portion of the bar during flood events. The size of these features ranges from less than 1 m to more than 10 m and reflects the diverse nature of alluvial depositional environments.

Perpendicular profiles are dramatically different than the parallel profiles. A large trough is present between 20 and 35 m on the St. Francois State Park profile, indicating the presence of a previous channel or flood chute in that location (Figure 33). Sigmoidal reflections across the length of the Morse Mill profile are indicative of lateral accretion deposits formed during point bar formation (Figure 34; Van Overmeeren, 1998; Bowling et al., 2005). Two reflections on the Cedar Hill profile can be seen at 5 and 10 m and possibly represent scoured areas (Figure 35; van Overmeeren, 1998).

Sediment Thickness

The thickness of alluvial deposits using GPR data were compared to refusal depths in the thalweg of the channel determined using a tile probe. The thalweg was used because it is the

lowest point in the cross-section and would therefore represent the maximum depth of refusal. The thickness of sediment is relatively constant on both parallel GPR profiles. Reflections can be clearly seen to depths of 3.0 or 3.5 m at St. Francois State Park and up to 5 m at Morse Mill (Figure 31 and 32). Deeper reflections at Morse Mill between 35 and 55 m indicate a deeper deposit of gravel that is likely related to the topography of the bar, which is not corrected for in the profile. The maximum tile probe depth was 2.5 m below the surface of the bar at St. Francois State Park and approximately 2.0 m below the surface of the bar at Morse Mill.

Sediment thickness is variable across perpendicular profiles. Clear boundaries are present at approximately 4.5 m at Cedar Hill and approximately 5 m at St. Francois State Park (Figure 33 and 35). Depths at Morse Mill are not as clearly identified and range from approximately 3 m to as much as 7 m (Figure 34). Reflections beyond these depths are weaker and likely influenced by saturated conditions below the water table. Depth to gravel lag determined do not correlate to reflections in the GPR data.

Results of the GPR bar study conducted here are similar to a previous study at St. Francois State Park by the Missouri Department of Natural Resources (2007). Both studies used the same frequency? The 3.0-3.5 m bar thickness at St. Francois State Park is similar to results from previous GPR studies there that suggest bedrock is around 3 meters deep.

Applicability of Methods

Floodplain Stratigraphy

The most useful data collected on the floodplains came from the DCR measurements that were able to provide information at the greatest depth and with the most variability. DCR was able to identify the breaks between silt-loam and sandy/gravelly deposits along most profiles, verified by floodplain cores. Additionally, channel fill deposits were also apparent in some of the profiles indicating the channel avulsed in the past to its current location and further verified using the GPR measurements, even though they were shallow. Furthermore, the overall electrical resistivities of the floodplain sediments are highest at St. Francois State Park and decrease going downstream. This is indicative of a fining of the floodplain deposits in the downstream direction. While this pilot study identifies potential uses of combined DCR measurements for stratigraphic analysis in this setting, more detailed subsurface investigations of the deposits and grain-size distribution are necessary to verify these findings.

The combined DCR and GPR methods have the ability to make distinctions between coarse textural changes within the floodplain sediments within the top 2-3 m of the surface. Given the high electrical resistivities, GPR data using 100 and 250 MHz antenna did not image the bottom

of the floodplain deposits. However, they did provide an additional constraint in verifying several anomalies seen on the DCR models, such as in the channel fill mentioned above. Using a 25 or 50 MHz antenna might overcome these challenges.

Gravel Bar Composition and Geometry

The GPR measurements were able to determine the total thickness of the bar material that was similar to a previous study conducted at St. Francois State Park. However, results from the GPR measurements on the gravel bars correlate poorly with tile probe depths collected at these locations. The major cause of discrepancies between GPR data and tile probe data is likely the inability of the tile probe to penetrate beyond large clasts below the surface of the bar. The tile probe may represent the minimal depth of the active deposit. Additionally, the saturation of sediment influences its reflectance and because water table elevations across the bars at all of the sites were unknown, the depth at which it influences the GPR data also remains unknown.

CONCLUSIONS

There are 6 main conclusions of this study.

1. The GPR and DCR methods used in this study were not able to discriminate between contaminated and uncontaminated sediment boundaries as determined by the floodplain core analysis.

2. DCR data of floodplain deposits has proven useful in determining the thickness of floodplain sediments and variations in the sedimentology of the floodplains. This method imaged the depth of the finer-grained silt-loam layer above the sand and gravel layers below. In most cases DCR was able to image the top of the coarse gravel lag deposits below the sandy layers above. The exception was at St. Francois State Park where the floodplain had thicker accumulations of material over gravel lag. Here, DCR data did not image the maximum thickness everywhere, suggesting that a more powerful system with greater distances between the current electrodes is needed.

3. GPR measurements on the floodplains imaged the top of the sand deposits and the images in general followed the trend of the anomalies seen on the DCR models. This can be seen as higher electrical resistivity zones on the DCR models and were apparent on the GPR models as non-horizontal reflections deeper than the other reflections.

4. DCR measurements have the potential to detect textural changes in fine-grain floodplain deposits relating to variations in alluvial sedimentation along the Big River. The average

electrical resistivity of the floodplain deposits decreased downstream which may be caused by a fining of the sediments. More detail sediment size distributions are needed to confirm this finding.

5. DCR measurements have the potential to detect old channel fill areas within the floodplain showing the size, shape, and former position of the paleo-channel. These areas are potential zones of contaminated sediment storage. DCR data combined with sediment dating techniques could also prove useful in understanding hydrological changes at different timescales or climatic regimes.

6. GPR methods used on the gravel bar areas were not able to image a change at depths comparable to the tile probe methods. The GPR images were able to detect the thickness of the overall deposit varying between 2.5 to 3.5 meters, which is deeper than the tile probe depth. Bar thickness profiles detected at St. Francois State Park are similar to a previous study conducted at this location.

REFERENCES

Asprion U and Aigner T (1997) Aquifer architecture analysis using ground-penetrating radar: Triassic and Quaternary examples (S. Germany). Env Geol 31: 66-75.

Bowling, J.C., Rodriguez, A.B., Harry, D.L., and C. Zheng, 2005. Delineating Alluvial Aquifer Heterogeneity Using Resistivity and GPR Data. Ground Water Vol. 43, no. 6 pp 890-903.

Brown, B.L., 1981. Soil Survey of St. Francois County, Missouri. United States Department of Agriculture, Soil Conservation Service and Forest Service in cooperation with the Missouri Agricultural Experiment Station.

Conyers, L (2004) Ground-penetrating Radar for Archaeology. Altamira Press, Walnut Creek, CA.

Conyers, L (2006) Ground-Penetrating Radar Techniques to Discover and Map Historic Graves. Hist. Arch 40: 64-73.

Missouri Department of Natural Resources (2007) The estimated volume of mine-related benthic Sediment at two point bars in St. Francois State Park using ground penetrating radar and x-ray fluorescene. Missouri Dept. of Natural Resources, Field Services Div., 118pp.

Dominic DF, Egan K, Carney C, Wolfe PJ and Boardman MR (1995) Delineation of shallow stratigraphy using ground penetrating radar. J Appl Geophys 33: 167-175.

Engels S, and Roberts, M (2005) The architecture of prograding sandy-gravel beach ridges formed during the last Holocene highstand; southwestern British Columbia, Canada. J Sediment Res 75: 1052-64.

Harari Z (1996) Ground-Penetrating Radar (GPR) for imaging stratigraphic features and groundwater in sand dunes, J Appl Geophys 36: 43-52.

Hirsch M, Bentley L, and Dietrich P (2008) A comparison of electrical resistivity, ground penetrating radar and seismic refraction results at a river terrace site, JEEG 13: 325-333.

James, L.A., 1989. Sustained storage and transport of hydraulic gold mining sediment in the Bear River, California. Annals of the Association of American Geographers 79:570-592.

James, L.A., 1991. Quartz concentration as an index of sediment mixing: hydraulic mine-tailings in the Sierra Nevada, California. Geomorphology 4:125-144.

Jol HM and Smith DG (1991) Ground penetrating radar of northern lacustrine deltas: Can J Earth Sci 28: 1939-1947.

Knighton, A.D., 1989. River adjustment to changes in sediment load: the effects of Tin mining on the Ringarooma River, Tasmania, 1875-1984. Earth Surface Processes and Landforms 14:333-359.

Kostic, B, and Aigner, T (2007) Sedimentary architecture and 3D ground-penetrating radar analysis of gravelly meandering river deposits (Neckar Valley, SW Germany). Sedimentology 54: 789-808.

Leclerc, R, and Hickin E (2009) The internal structure of scrolled floodplain deposits based on ground-penetrating radar, North Thompson River, British Columbia. Geomorph 21: 17-38.

Loke M, and Barker R (1996) Rapid least-squares inversion of apparent resistivity pseudo-sections using quasi-Newton method. Geoph Pros 44: 131-152.

MacDonald D.D., C.G. Ingersoll, and T.A. Berger. 2000. Development and evaluation of consensus-based sediment quality guidelines for freshwater ecosystems. Arch. Environ. Contam. Toxicol. 39:20-31.

MDNR, 1979. Geologic Map of Missouri. Division of Geology and Land Survey of the Missouri Department of Natural Resources.

MDNR, 2001. Biological assessment and fine sediment study: Flat River (Flat River Creek), St. Francois County, Missouri. Prepared by the Water Quality Monitoring Section, Environmental Services Program, Air and Land Protection Division of the Missouri Department of Natural Resources.

MDNR, 2003. Biological assessment and fine sediment study: Big River (lower): Irondale to Washington State Park, St. Francois, Washington, and Jefferson Counties, Missouri. Prepared by the Water Quality Monitoring Section, Environmental Services Program, Air and Land Protection Division of the Missouri Department of Natural Resources.

MDNR, 2007 . The Estimated Volume of Mine-Related Benthic Sediment in Big River at Two Point Bars in St. Francois State Park Using Ground Penetrating Radar and X-Ray Flourescence.

Prepared by the Water Quality Monitoring Unit, Environmental Services Program, Field Services Division of the Missouri Department of Natural Resources.

Neal A (2004) Ground-penetrating radar and its use in sedimentology; principles, problems and progress. Earth-Science Rev 66: 261-330.

Newfields, 2006. Hydrogeology and groundwater quality of mill waste piles: St. Francois County, Missouri. Report submitted on November 30, 2006 as an addendum to the March 2006 ―Focused Remedial Investigation of Mined Areas in St. Francois County, Missouri‖ by Newfields, 730 17th Street, Suite 925, Denver, CO 80202.

Regli C, Huggenberger P and Rauber M (2002) Interpretation of drill core and georadar data of coarse gravel deposits. J Hydology 255: 234-252.

Reynolds JM (1997) An Introduction to Applied and Environmental Geophysics. John Wiley & Sons 796 pp.

Roberts MC, Bravard JP and Jol HM (1997) Radar signatures and structure of an avulsed channel: Rhone River, Aoste, France. J Quat Sci 12: 35-42.

Roberts, A.D., D.E. Mosby, J.S. Weber, J. Besser, J. Hundley, S. McMurray, and S. Faiman,S., 2009. An assessment of freshwater mussel (Bivalvia Margaritiferidae and Unionidae) populations and heavy metal sediment contamination in the Big River, Missouri. Report prepared for U.S. Department of the Interior, Washington D.C.

Rosgen, D., 2006. Watershed assessment of river stability and sediment supply (WARSSS). Wildland Hydrology, Fort Collins, Colorado.

Schmitt, C.J., S.E. Finger, T.W. May, M.S. Kaiser, M.S., 1987, Bioavailability of lead and cadmium from mine tailings to the pocketbook mussel (*Lampsilis ventricosa*), *in* Neves, R.J., ed., Proceedings of the Workshop on Die-offs of Freshwater Mussels in the United States: Rock Island, Illinois, U.S. Fish and Wildlife Service and Upper Mississippi River Conservation Committee, p. 115−142.

Smith, B.J., and J.G. Schumacher, 1993. Surface-water and sediment quality in the Old Lead Belt, southeastern Missouri—1988-89. USGS Water-Resources Investigations Report 93-4012.

van Overmeeren (1998) Radar facies of unconsolidated sediments in The Netherlands: A radar stratigraphy interpretation method for hydrogeology. J App Geophys 40: 1-18.

Table 1. Site Characteristics

Site #	Site Name	County	State Plan Coordinates Missouri East x (feet)	y (feet)	A_d km^2	Elevation m	Distance km	Valley Width km
M-7	St. Francois State Park	St. Francois	808,839.05110	772,269.44002	1,007	191	140.8	0.1
M-14	Washington State Park	Jefferson	767,864.30554	820,675.37368	1,363	169	101.7	0.6
M-18	Morse Mill Park	Jefferson	776,379.20859	888,708.58890	2,165	144	49.8	0.9
M-19	Cedar Hill Park	Jefferson	779,681.95886	915,698.25127	2,296	138	32.7	1.0

Table 2. Summary of Bar Characteristics

Site #	Site Location	Bar Length m	Bar Width m	Max Bar Thickness m	%< 2mm m	% > 16mm m	Mean Pb Concentration (<2mm) mg/kg
M-7	St. Francois State Park	150	20	2.5	49	9	1,027
M-18	Morse Mill Park	88	17	2	32	18	237
M-19	Cedar Hill Park	100	36	?	56	19	321

Table 3. Typical Depths and Concentrations of Floodplain Features

Site #	Site Location	Floodplain Unit	Depth to Sand/Gravel m	Depth to Coarse Gravel Lag m	Contamination Depth m	Peak Contamination Depth m	Mean Pb Concentration ppm	Max Pb Concentration ppm
M-7	St. Francois State Park	Near Channel	3.9	7.6	6	3.8	1,673	5,542
		Floodplain	4.5	7.6	1.5	1.1	2,837	7,287
M-14	Washington State Park	Near Channel	4.1	6.3	3.6	1.4	1,206	2,220
		Floodplain	4	7.4	2.1	1	1,644	12,307
		Backswamp	2.8	4.9	0.9	0.7	832	4,426
M-18	Morse Mill Park	Near Channel	3.6	?	2.6	1	1,581	6,526
		Floodplain	2.4	?	1.2	0.8	682	1,350
M-19	Cedar Hill Park	Near Channel	?	?	3.6	1.7	1,160	3,229
		Floodplain	?	?	0.4	0.2	278	781

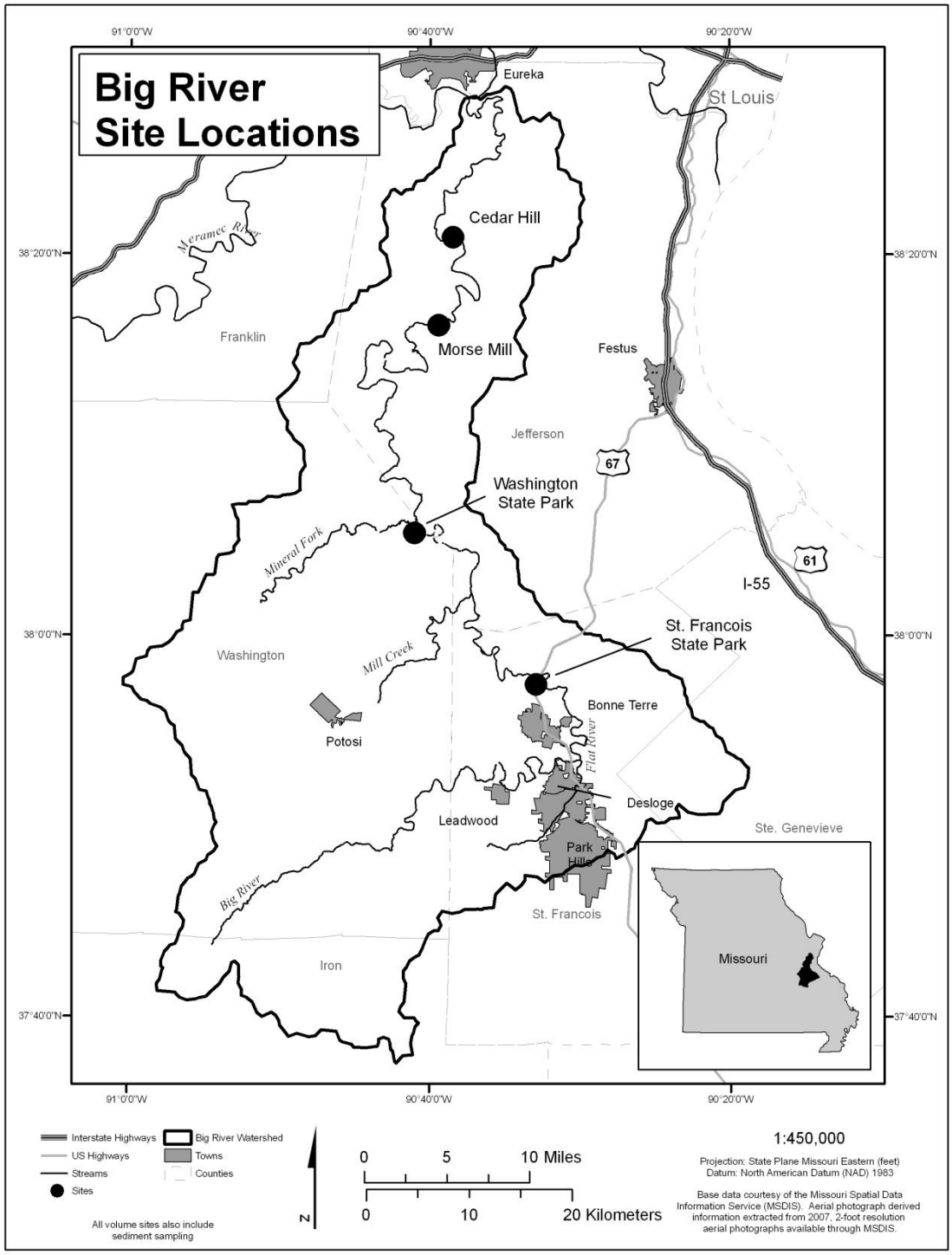

Figure 1. Location of the Big River watershed in eastern Missouri. The black circles are the locations of the geophysical surveys from north to south, respectively: Cedar Hill, Morse Mill, Washington State Park and St. Francois State Park.

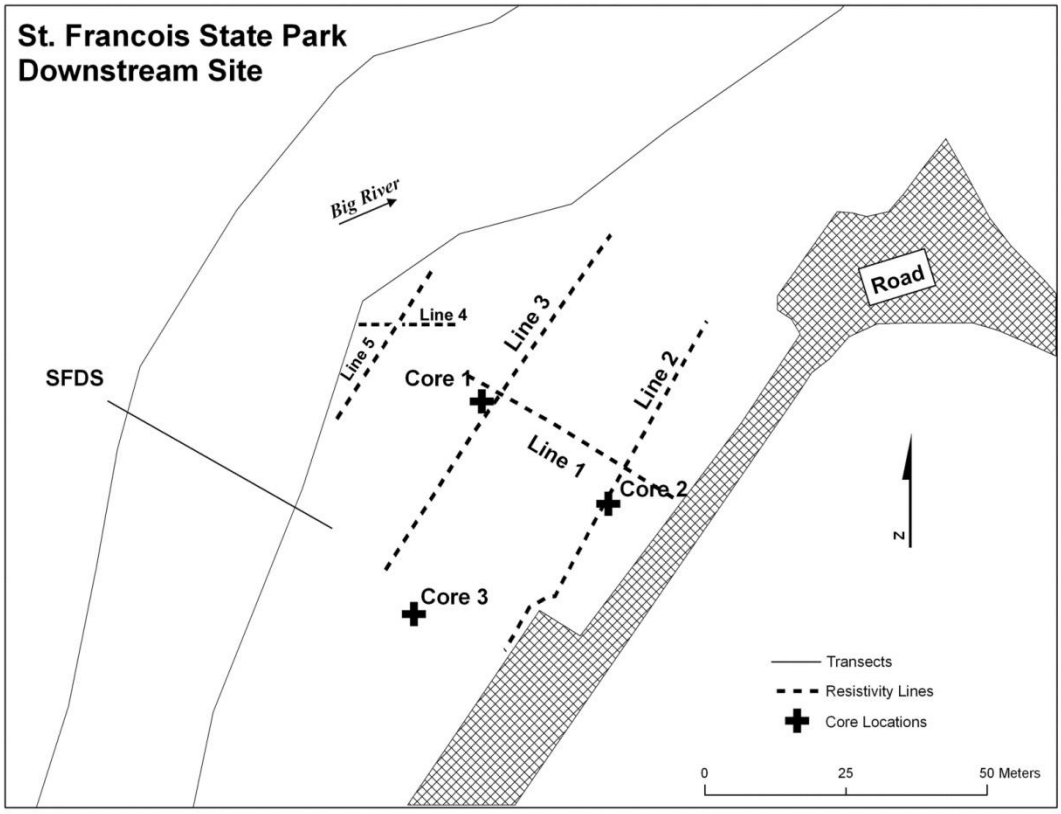

Figure 2. Location of the geophysical profiles and drill holes at St. Francois State Park.

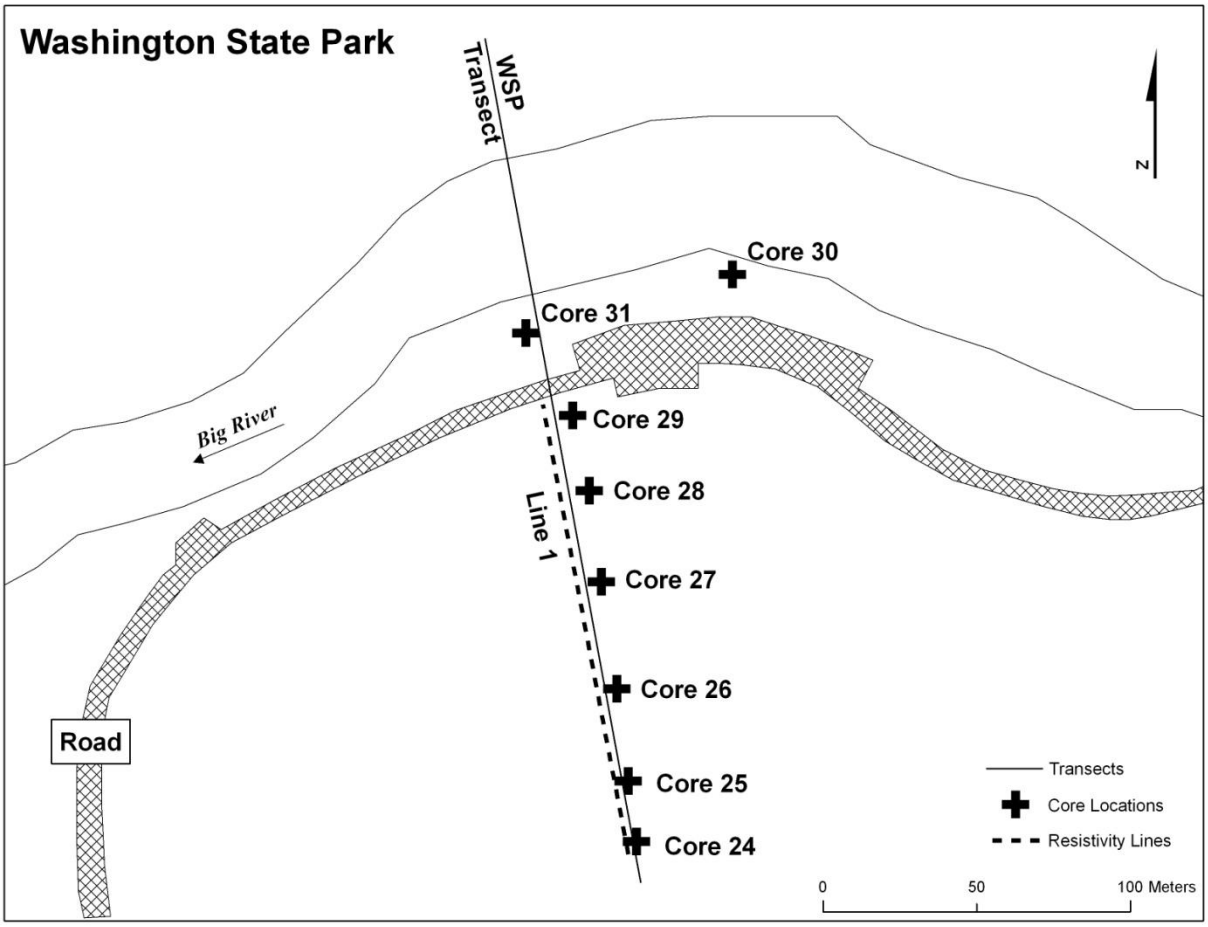

Figure 3. Location of the geophysical profiles and drill holes at Washington State Park.

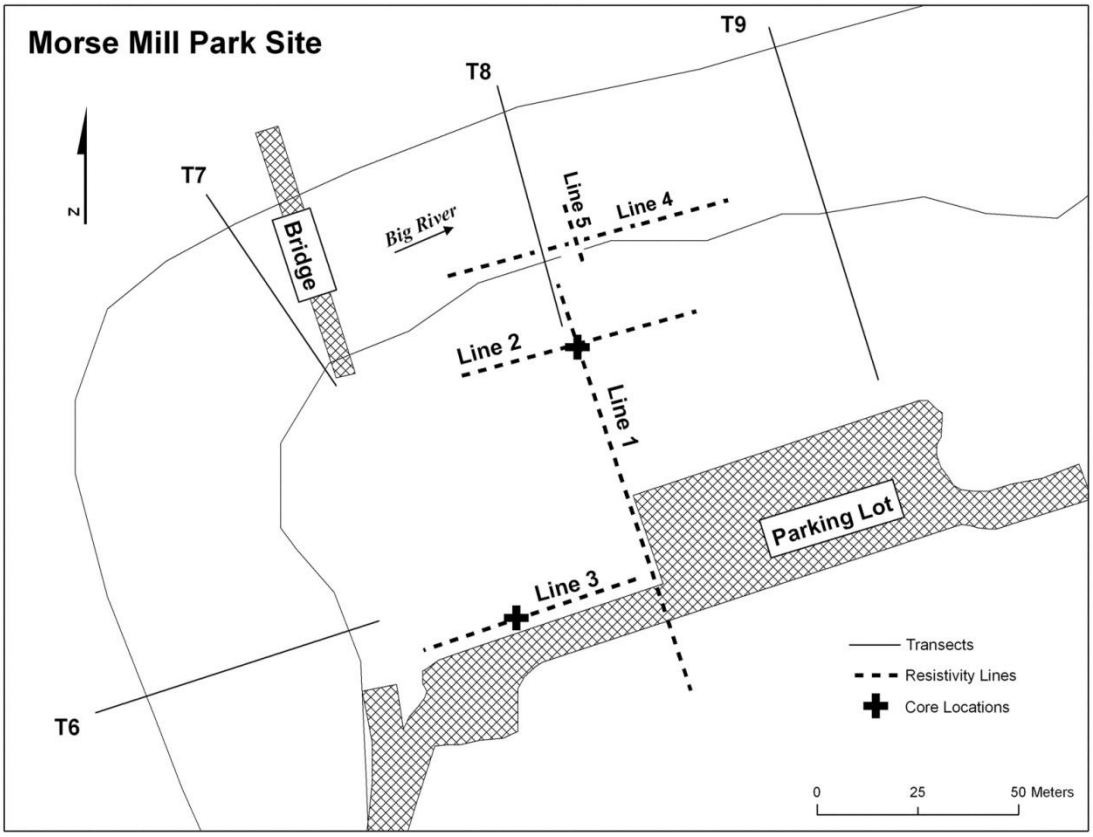

Figure 4. Location of the geophysical profiles and drill holes at Morse Mill County Park

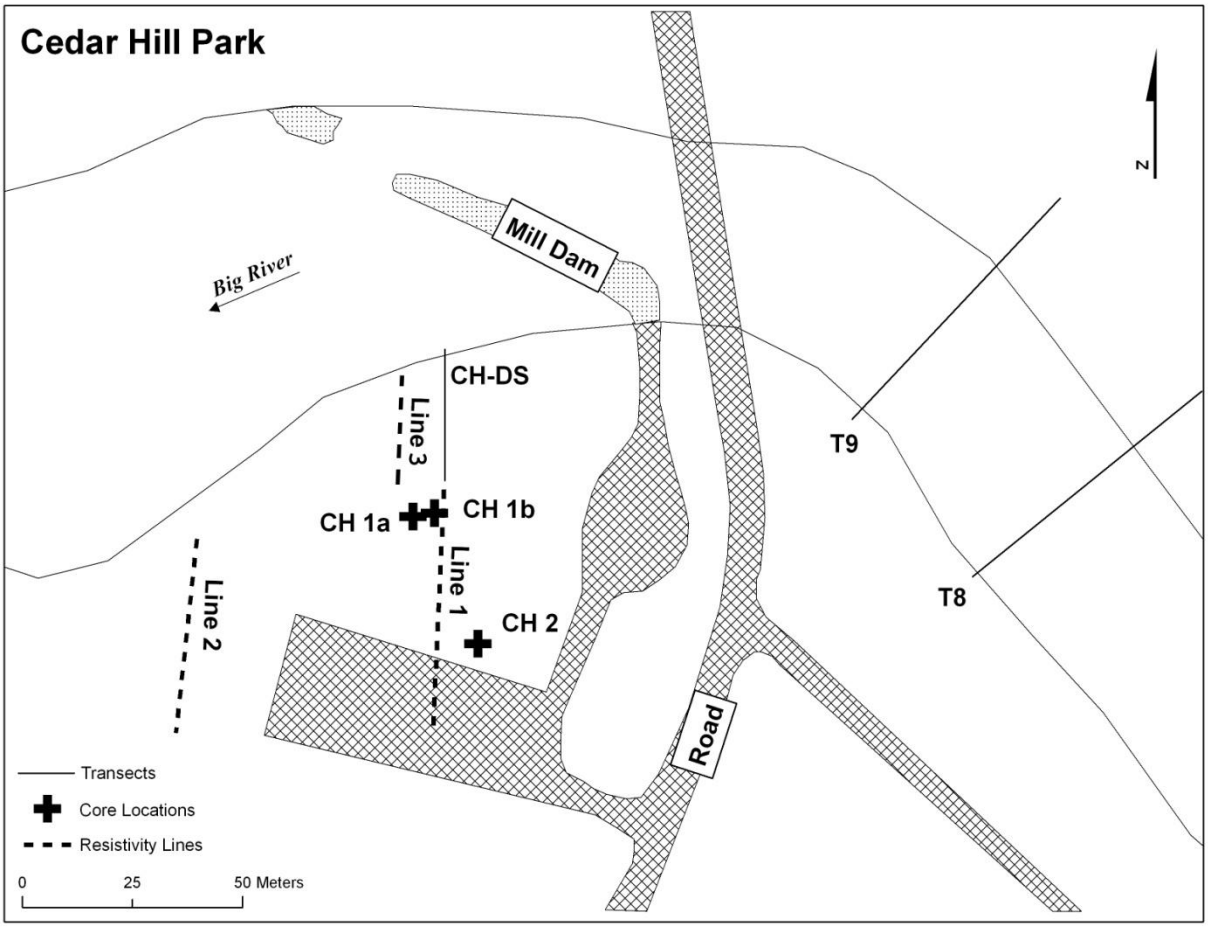

Figure 5. Location of the geophysical profiles and drill holes at Cedar Hill County Park

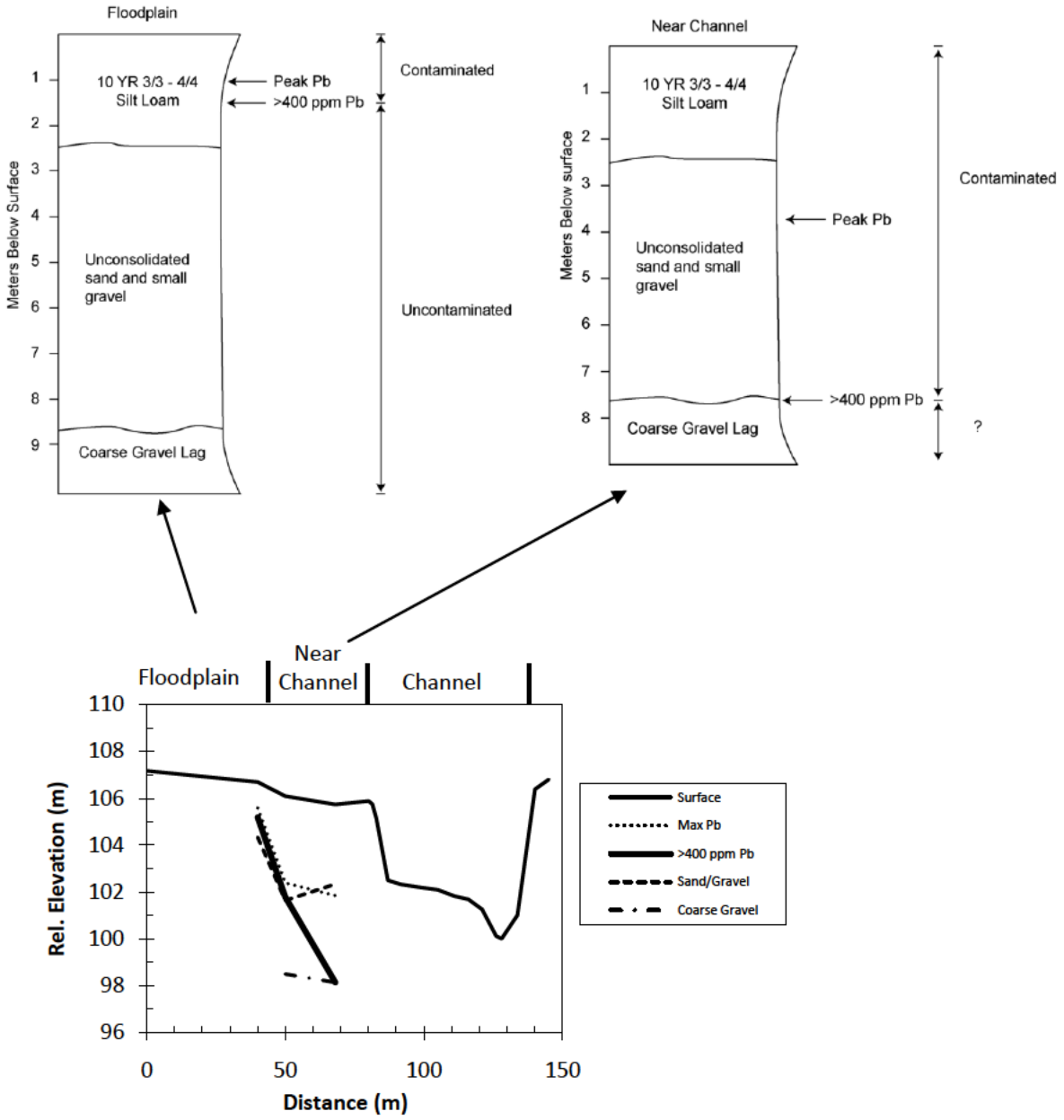

Figure 6. St. Francois State Park cross-section with stratigraphy and contamination profiles of floodplain and near channel overbank deposits

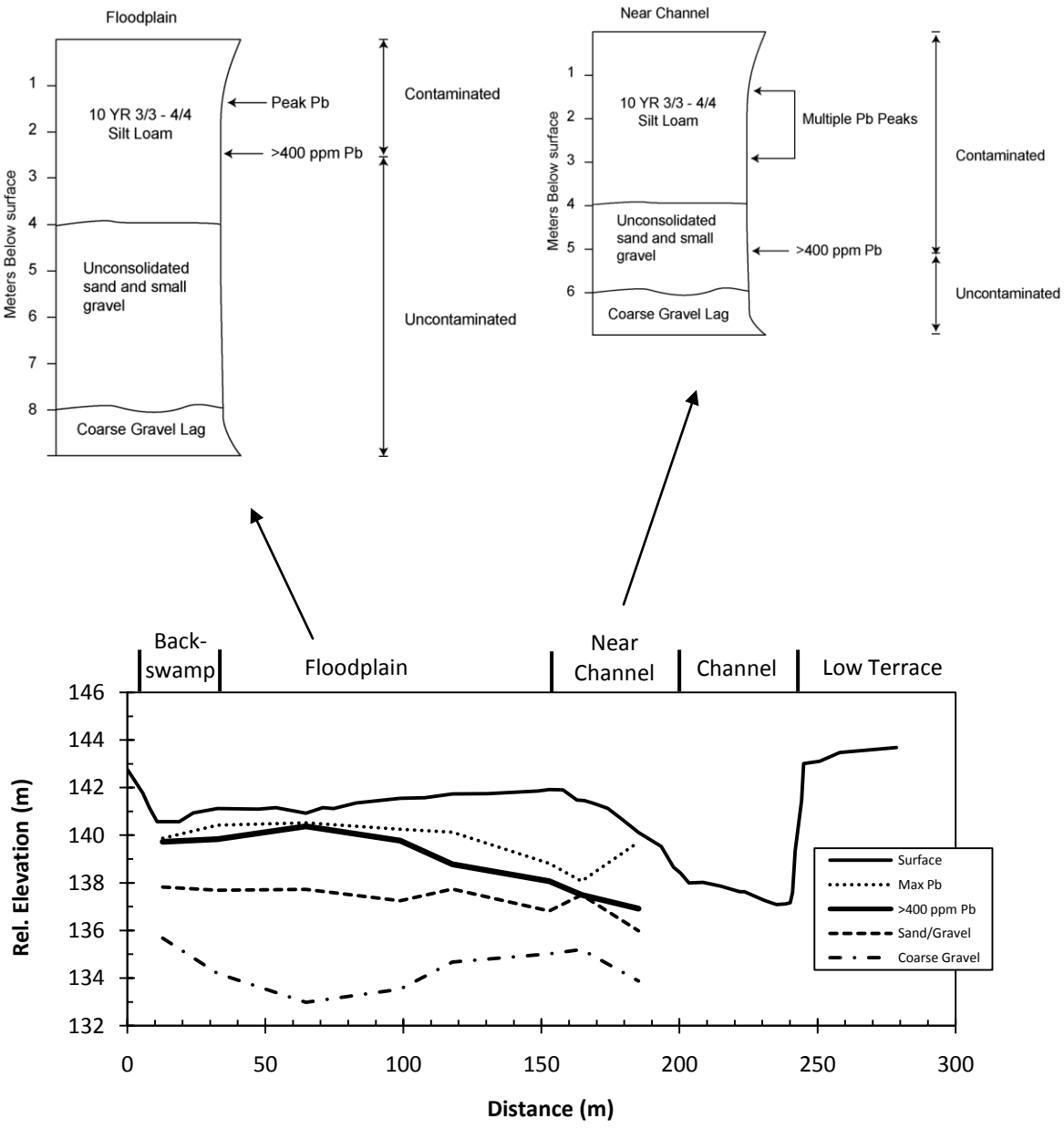

Figure 7. Washington State Park cross-section with stratigraphy and contamination profiles of floodplain and near channel overbank deposits

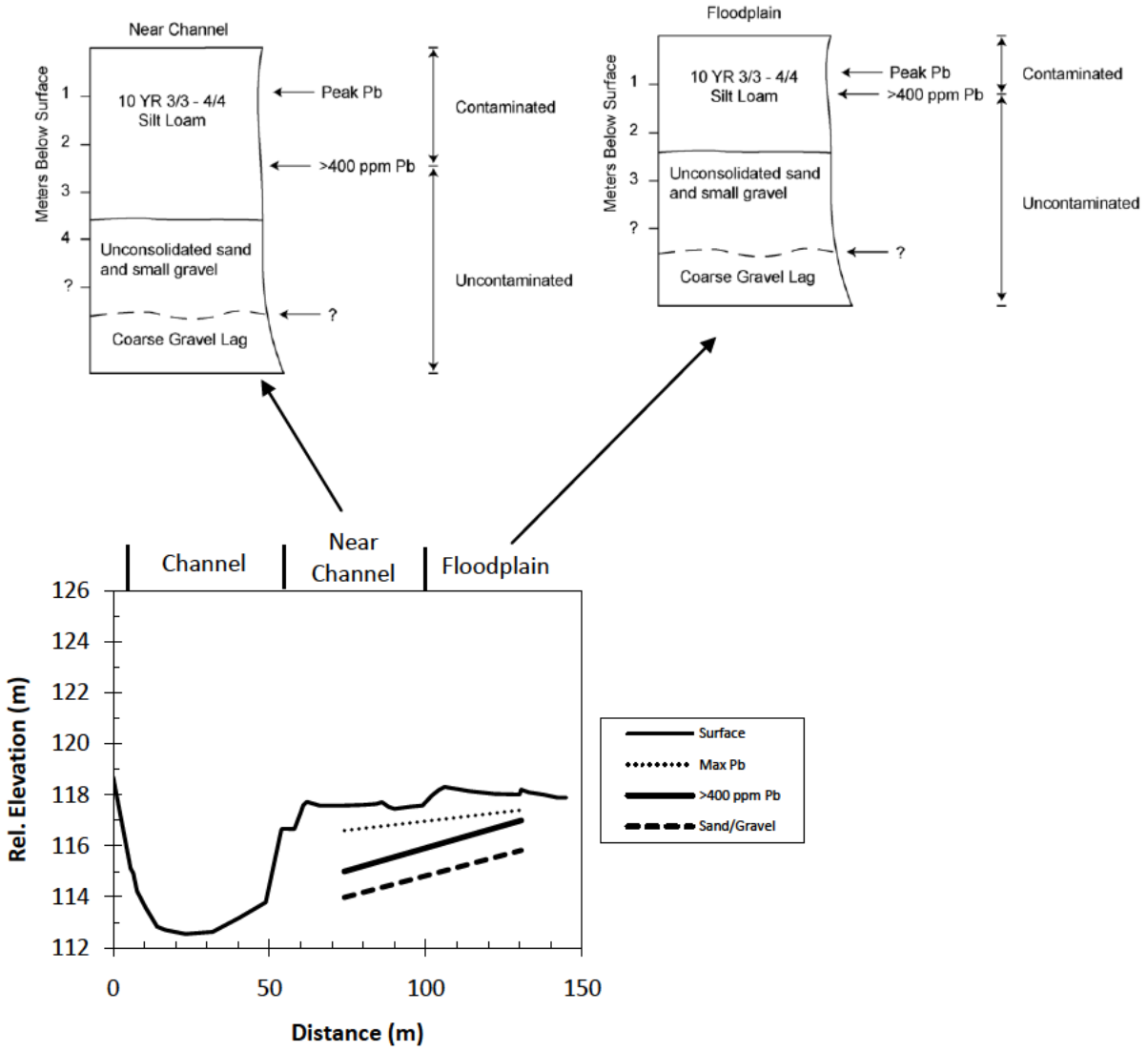

Figure 8 Morse Mill cross-section with stratigraphy and contamination profiles of floodplain and near channel overbank deposits

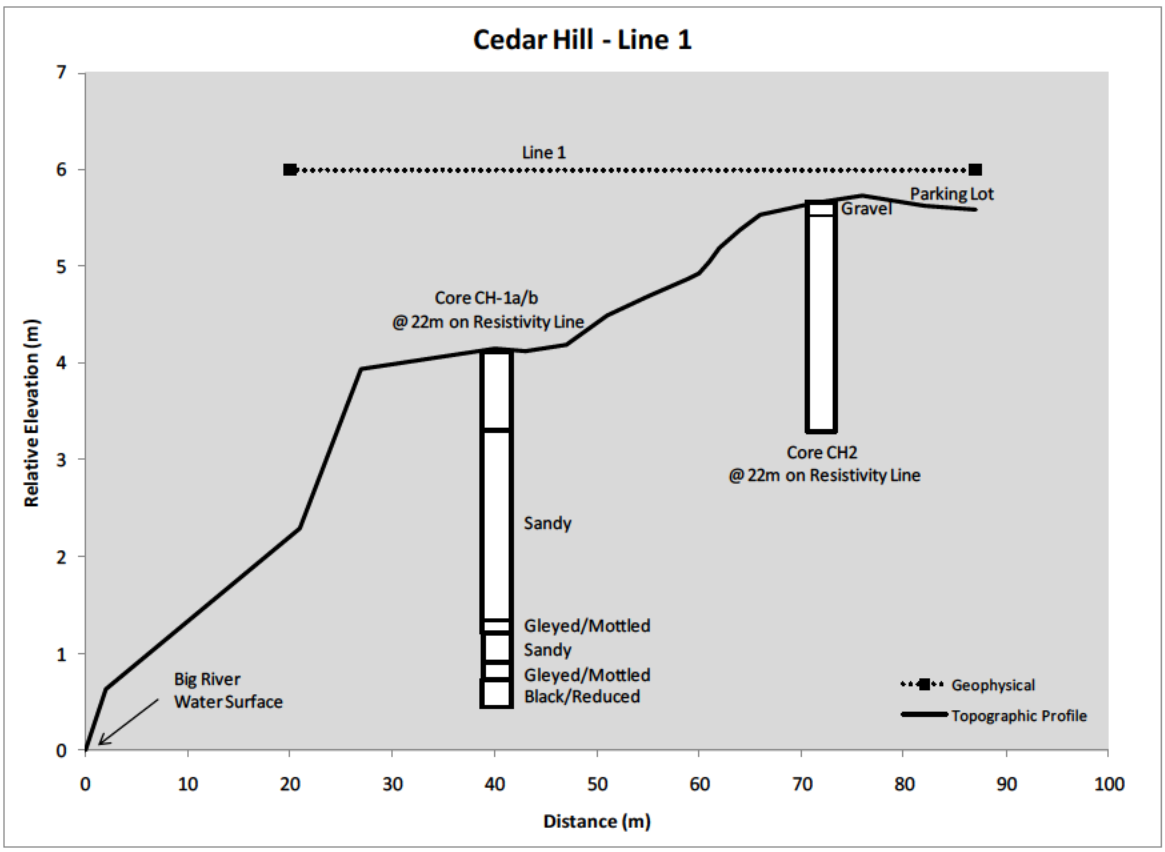

Figure 9. Cedar Hill Park

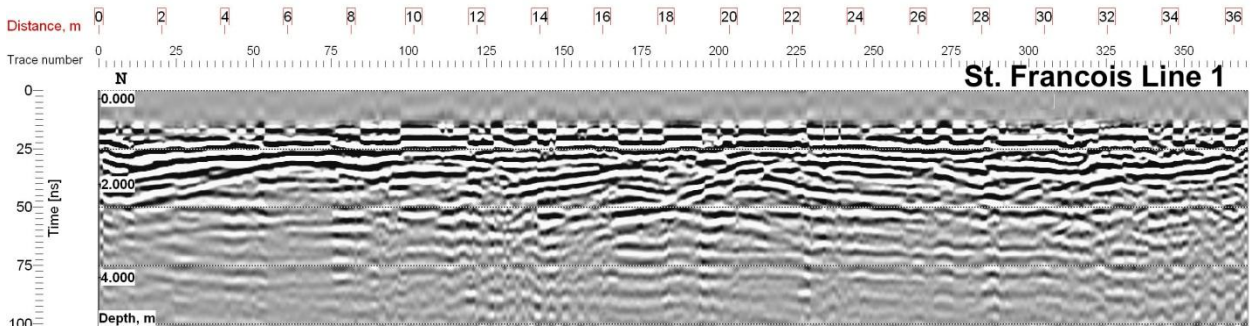

Figure 10. Processed 250 MHz GPR profile along line 1 perpendicular to the Big River at St. Francois State Park.

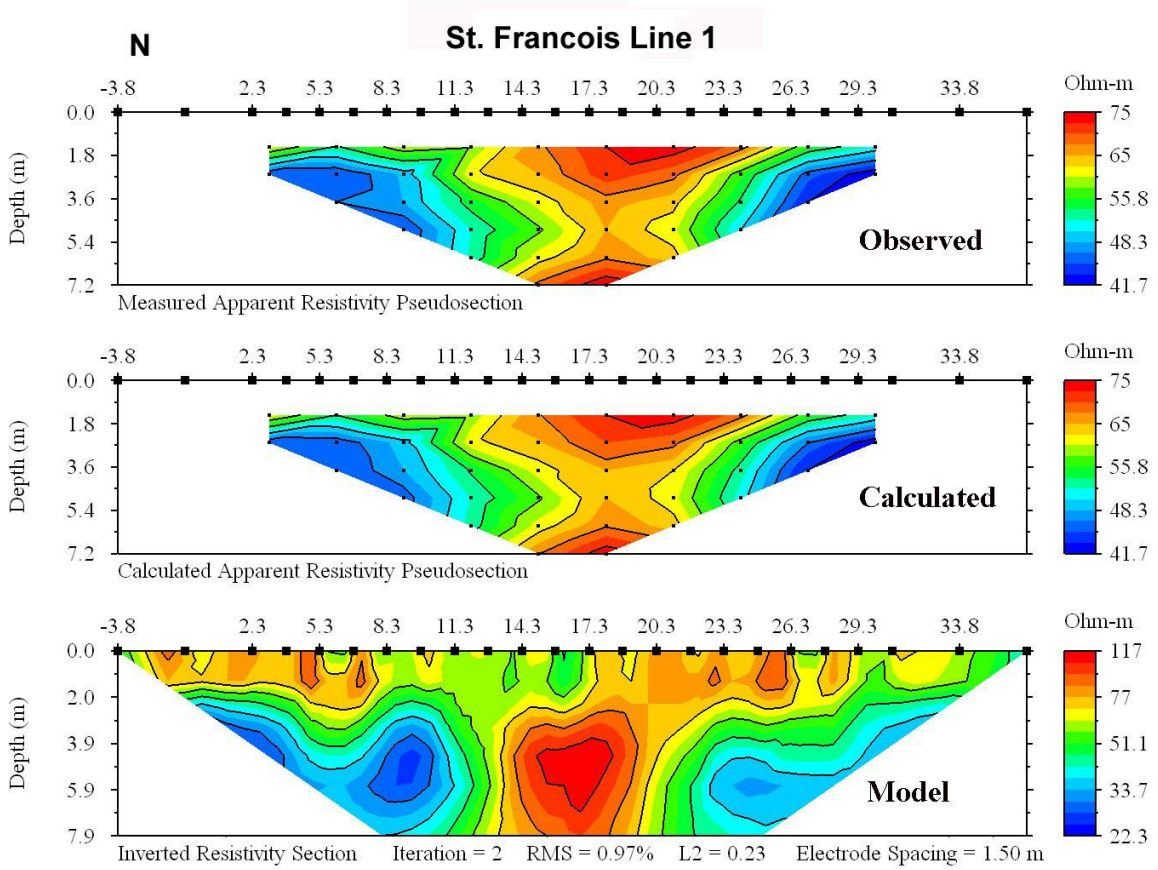

Figure 11. Two-dimensional resistivity model with the observed and calculated data along profile 1 at St. Francois State Park.

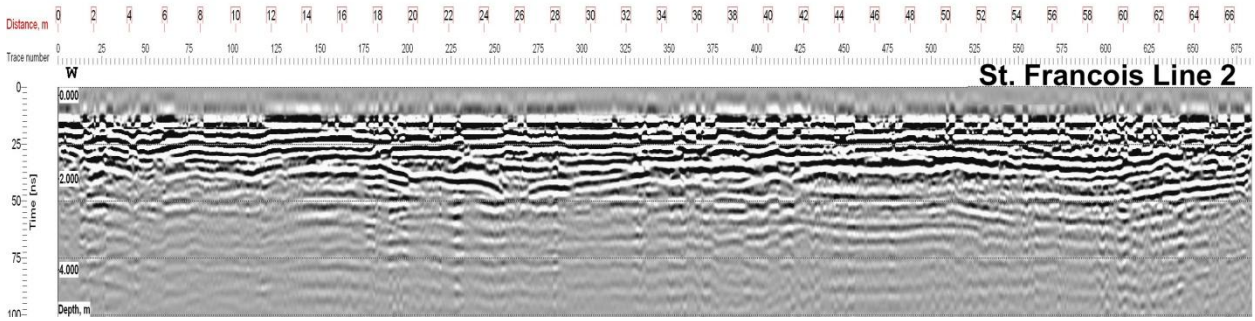

Figure 12. Processed 250 MHz GPR profile along line 2 parallel to the Big River at St. Francois State Park.

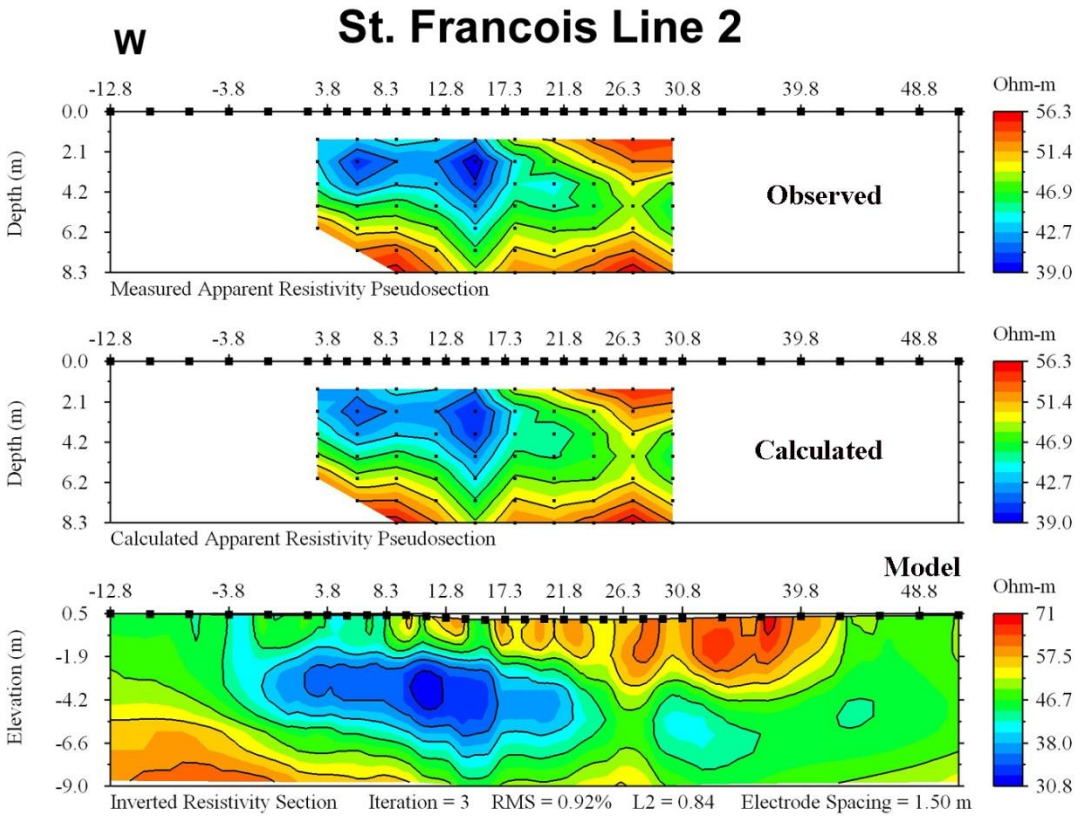

Figure 13. Two-dimensional resistivity model with the observed and calculated data along profile 2 at St. Francois State Park.

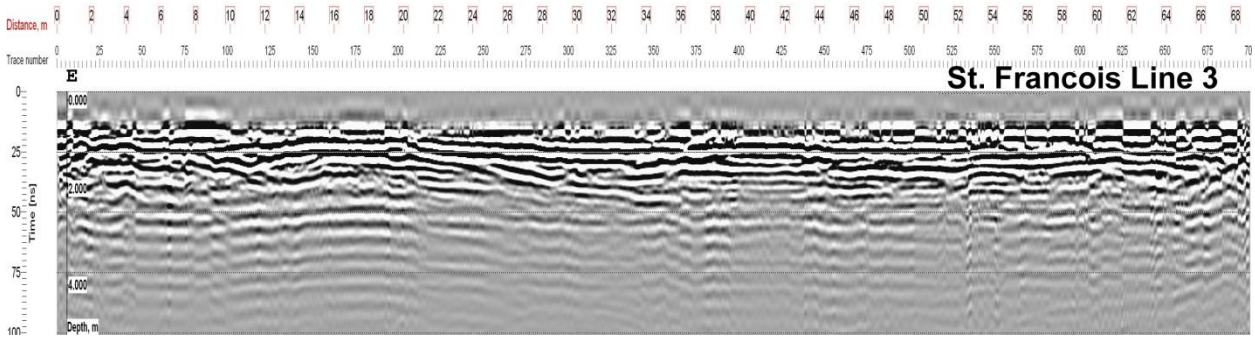

Figure 14. Processed 250 MHz GPR profile along line 3 parallel to the Big River at St. Francois State Park.

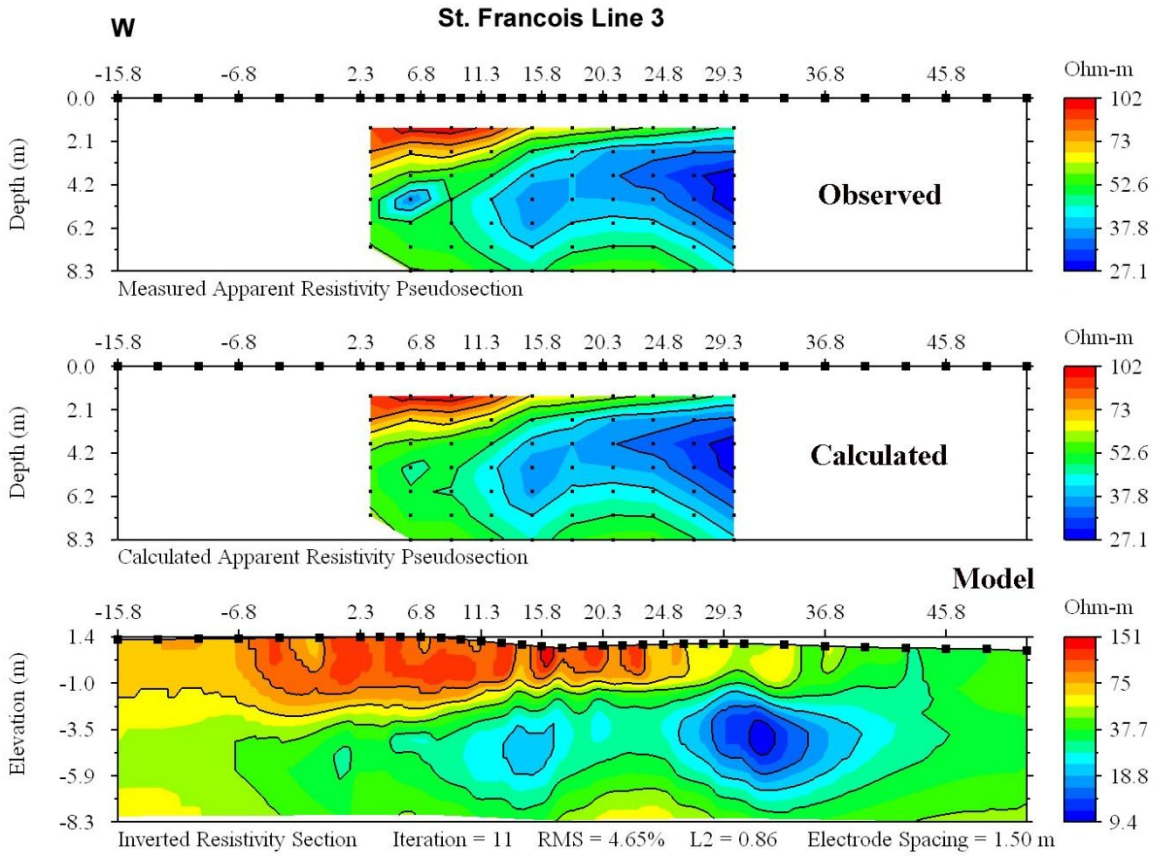

Figure 15. Two-dimensional resistivity model with the observed and calculated data along profile 3 at St. Francois State Park.

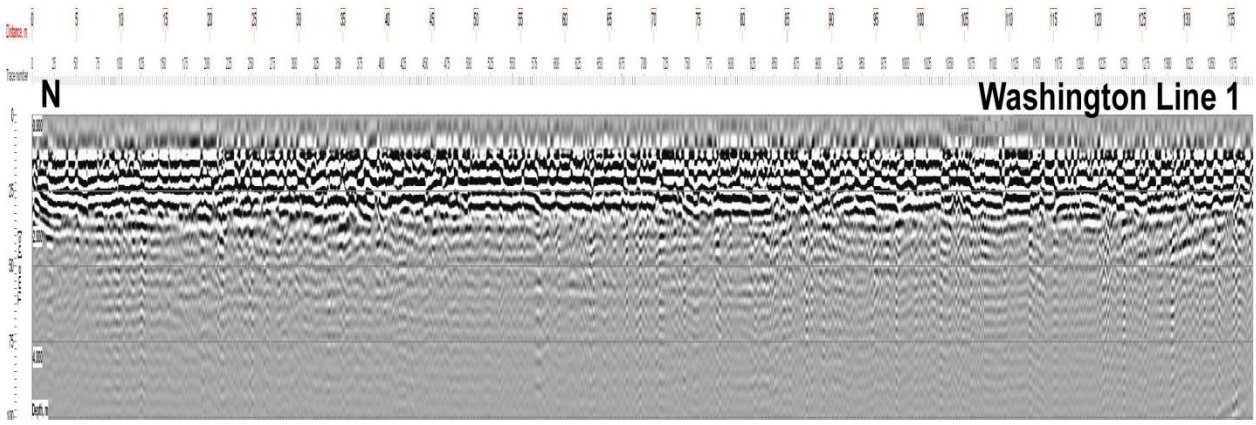

Figure 16. Processed 250 MHz GPR profile along line 1 perpendicular to the Big River at Washington State Park.

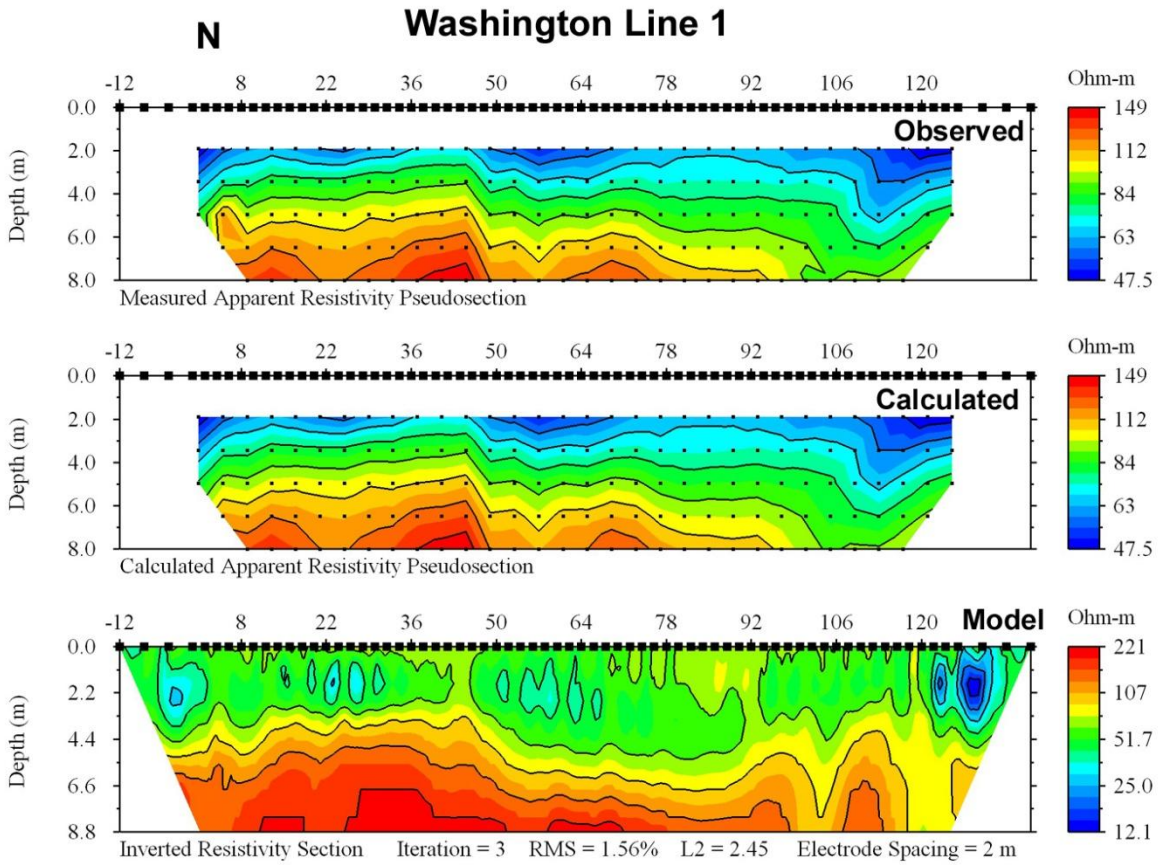

Figure 17. Two-dimensional resistivity model with the observed and calculated data along profile 1 at Washington State Park.

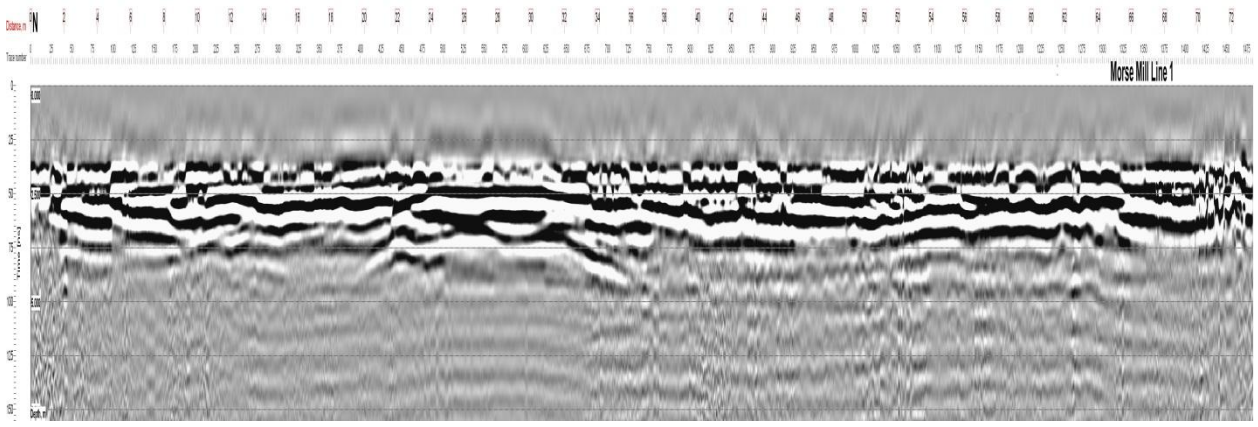

Figure 18. Processed 250 MHz GPR profile along line 1 perpendicular to the Big River at Morse Mill.

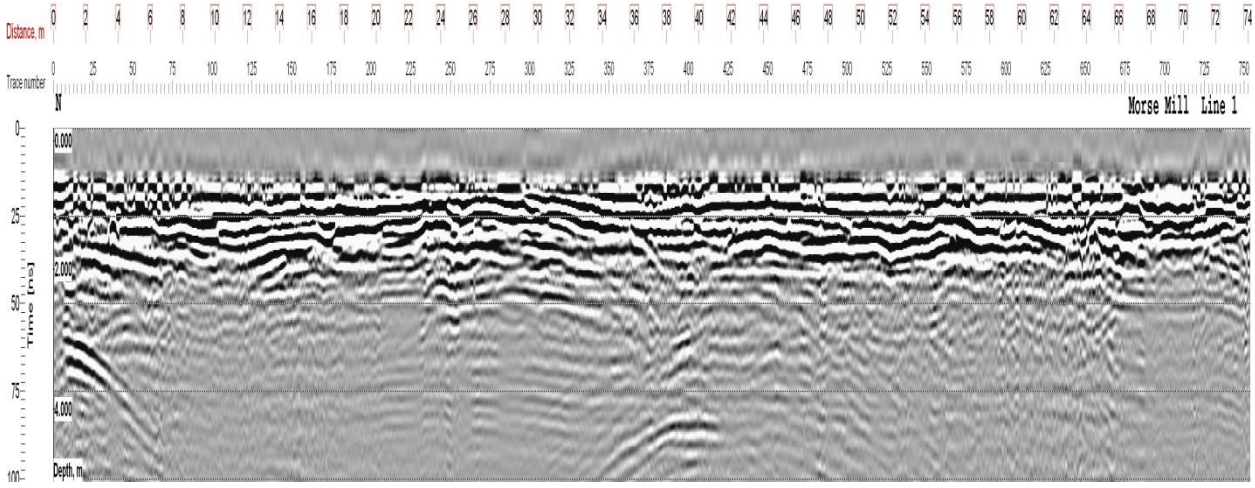

Figure 19. Processed 100 MHz GPR profile along line 1 perpendicular to the Big River at Morse Mill.

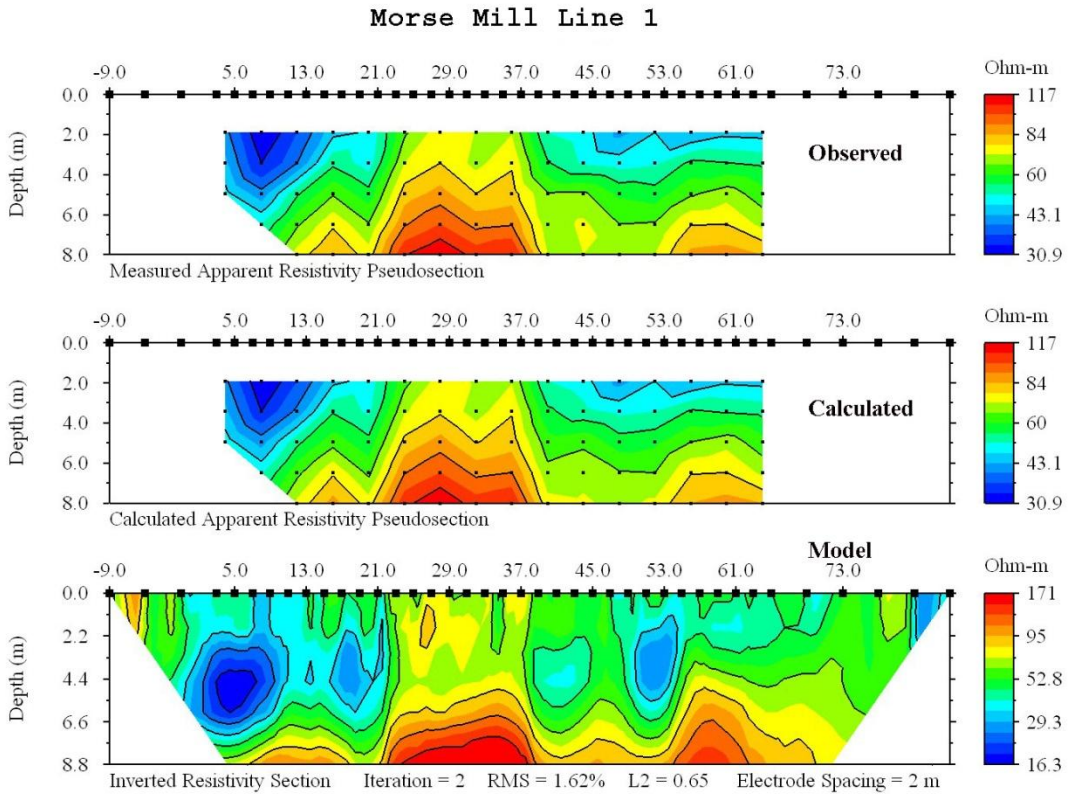

Figure 20. Two-dimensional resistivity model with the observed and calculated data along profile 1 at Morse Mill.

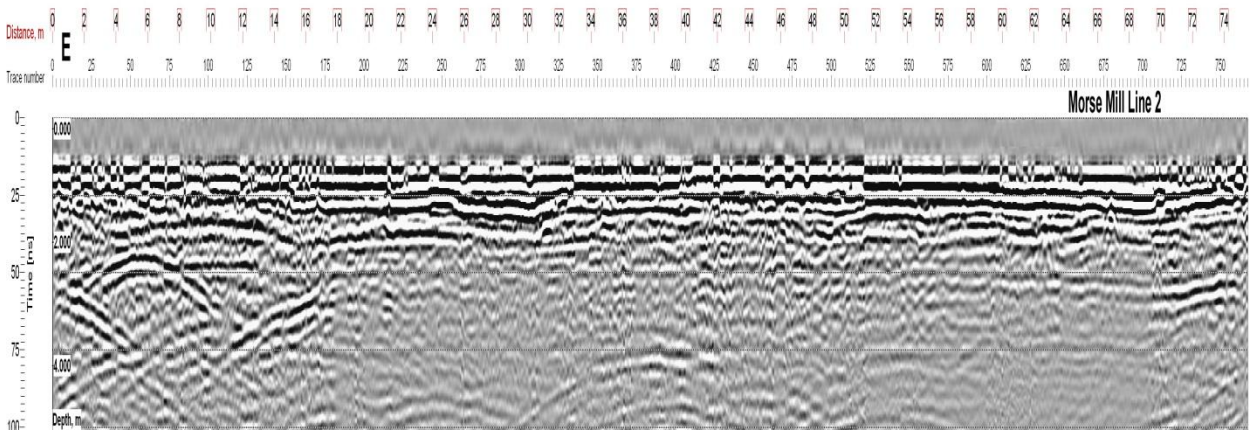

Figure 21. Processed 250 MHz GPR profile along line 2 parallel to the Big River at Morse Mill.

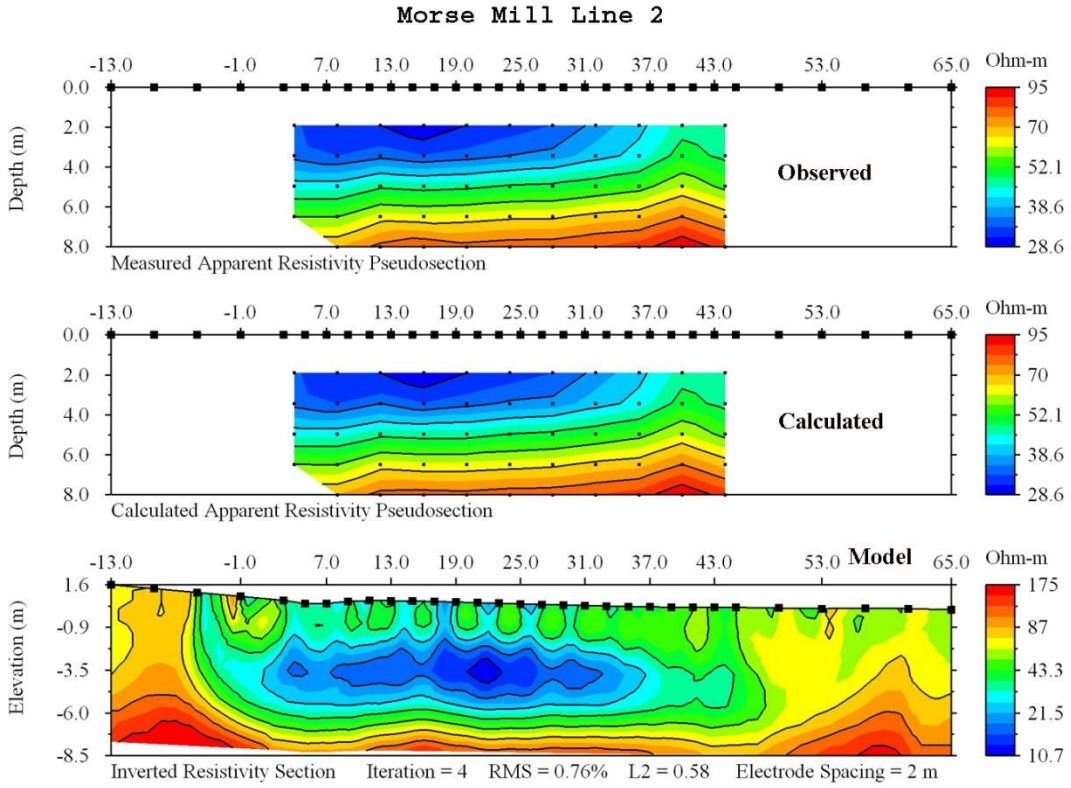

Figure 22. Two-dimensional resistivity model with the observed and calculated data along profile 2 at Morse Mill.

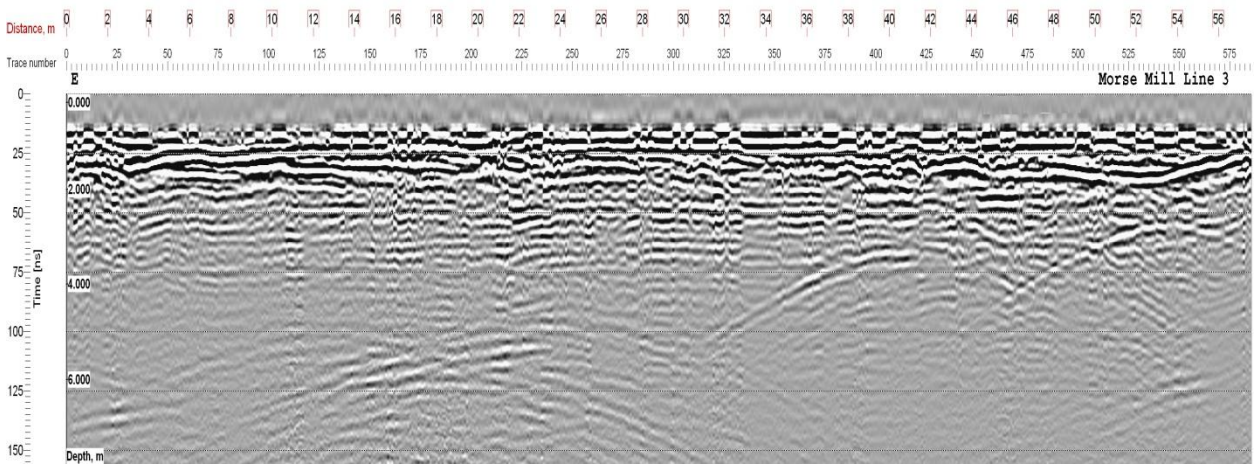

Figure 23. Processed 250 MHz GPR profile along line 3 parallel to the Big River at Morse Mill.

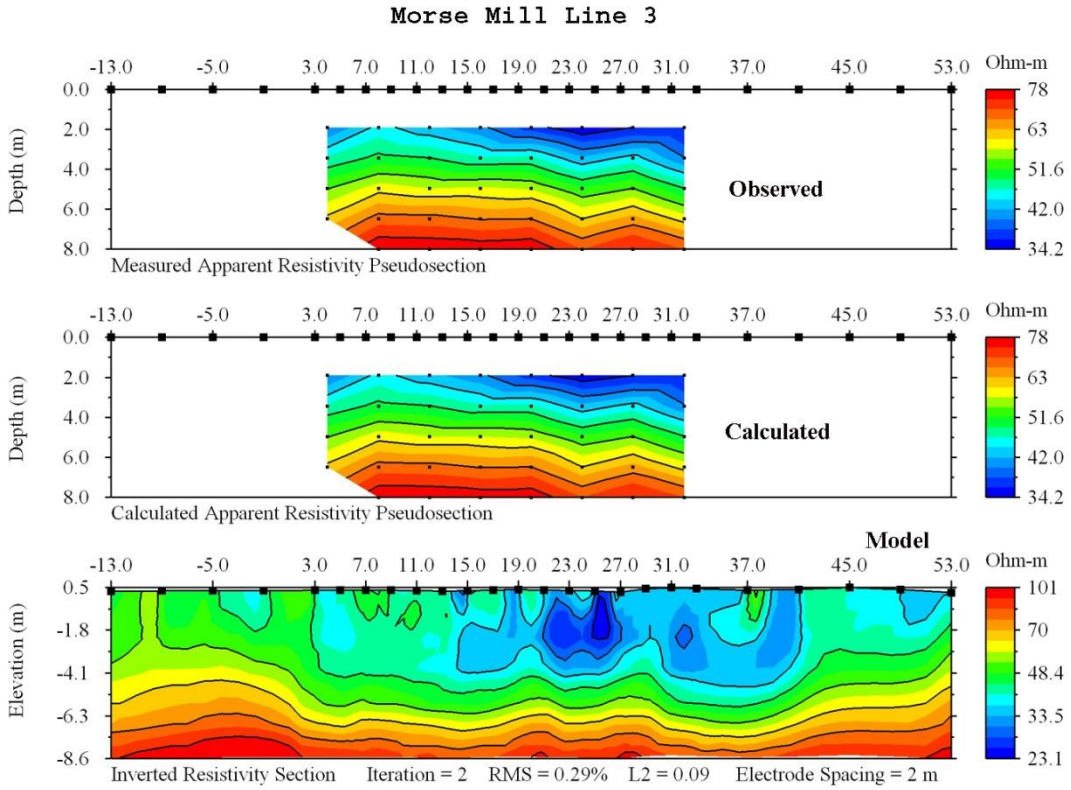

Figure 24. Two-dimensional resistivity model with the observed and calculated data along profile 3 at Morse Mill.

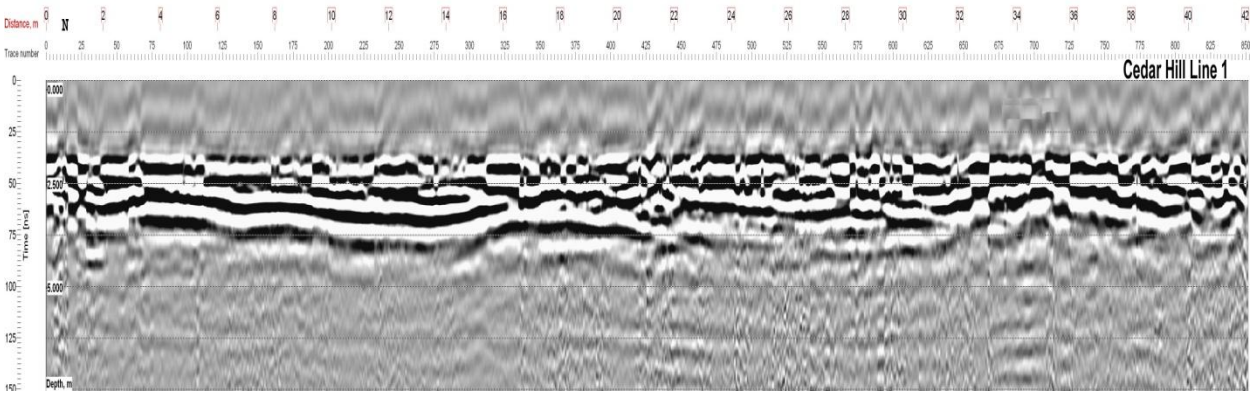

Figure 25. Processed 100 MHz GPR profile along line 1 perpendicular to the Big River at Cedar Hill.

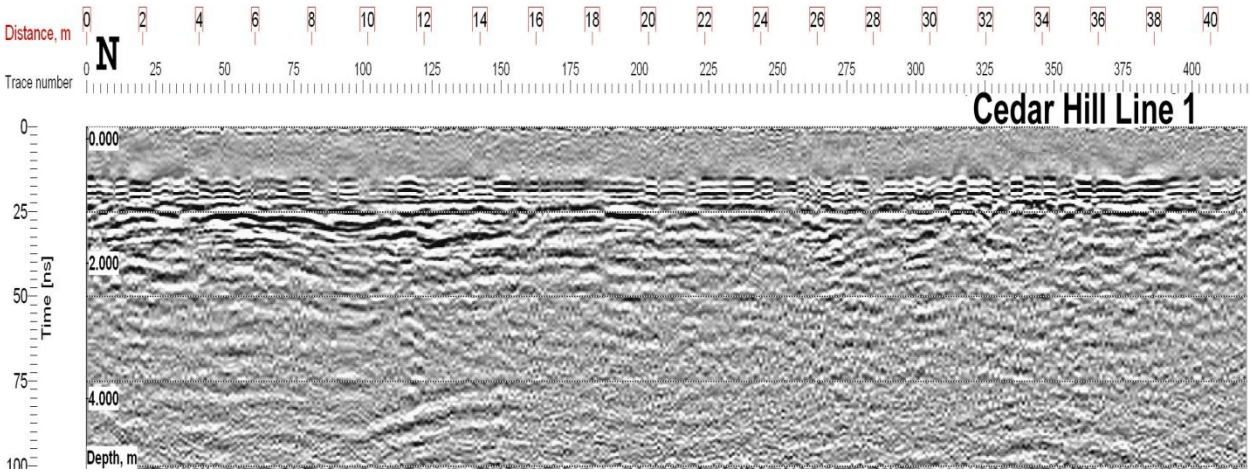

Figure 26. Processed 250 MHz GPR profile along line 1 perpendicular to the Big River at Cedar Hill.

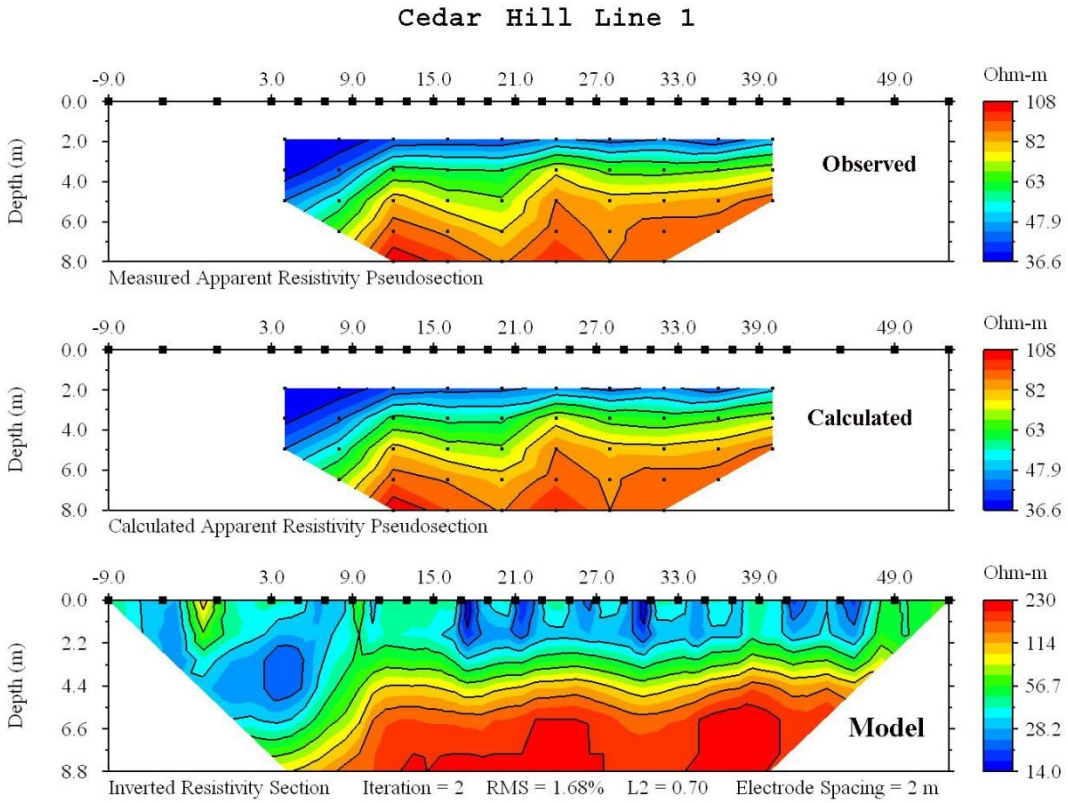

Figure 27. Two-dimensional resistivity model with the observed and calculated data along profile 1 at Cedar Hill.

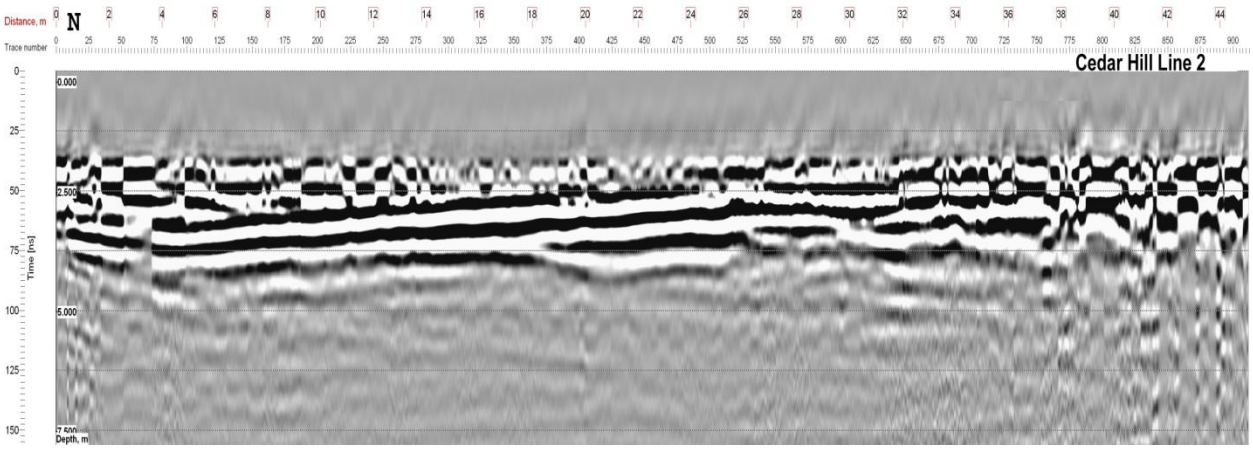

Figure 28. Processed 100 MHz GPR profile along line 2 perpendicular to the Big River at Cedar Hill.

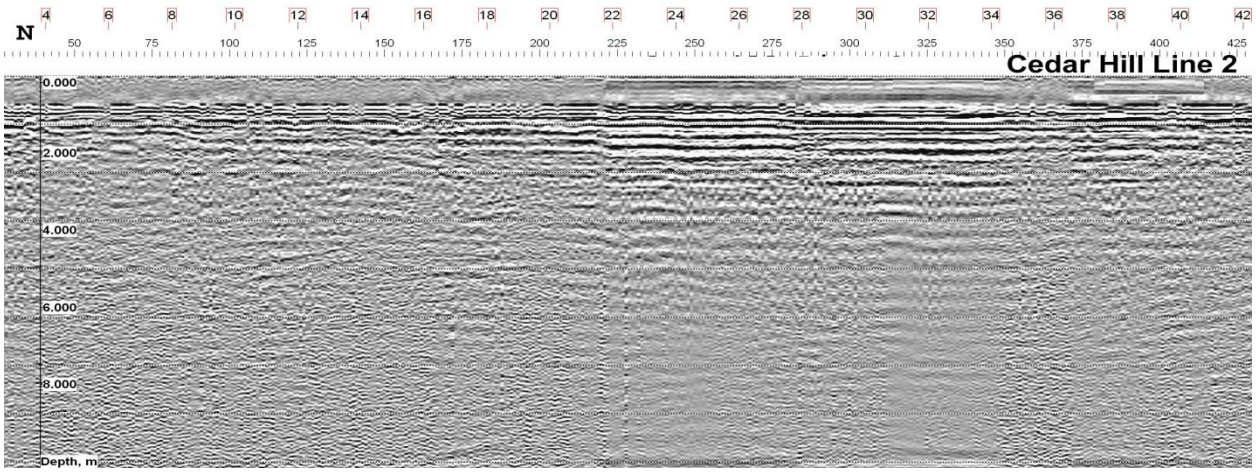

Figure 29. Processed 250 MHz GPR profile along line 2 perpendicular to the Big River at Cedar Hill.

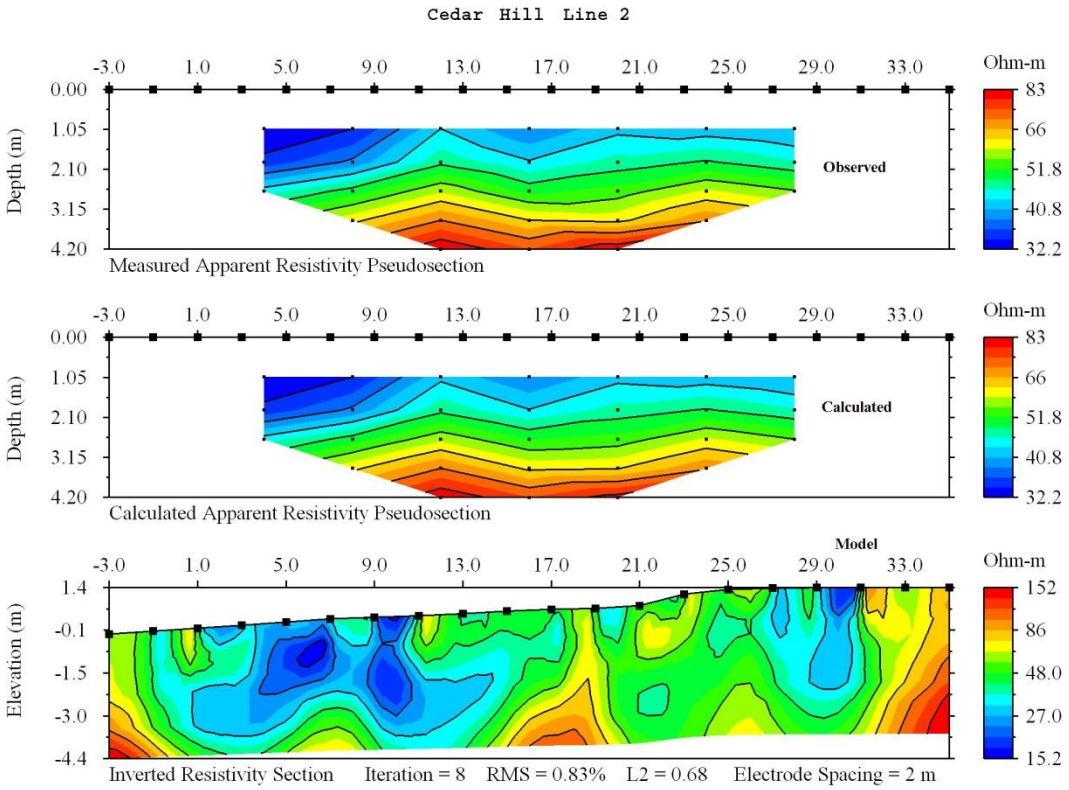

Figure 30. Two-dimensional resistivity model with the observed and calculated data along profile 2 at Cedar Hill.

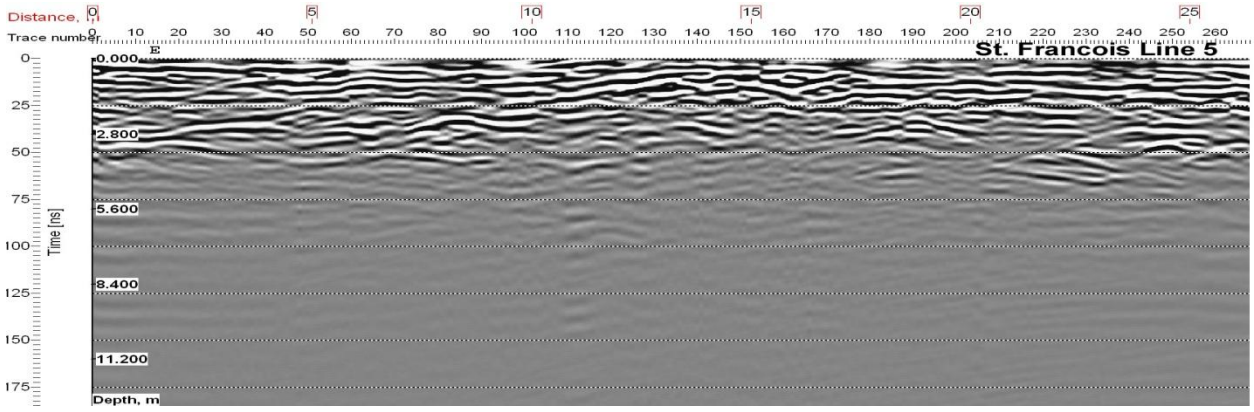

Figure 31. Processed 250 MHz GPR profile along line 5 parallel to the Big River across the gravel bar at St. Francois State Park.

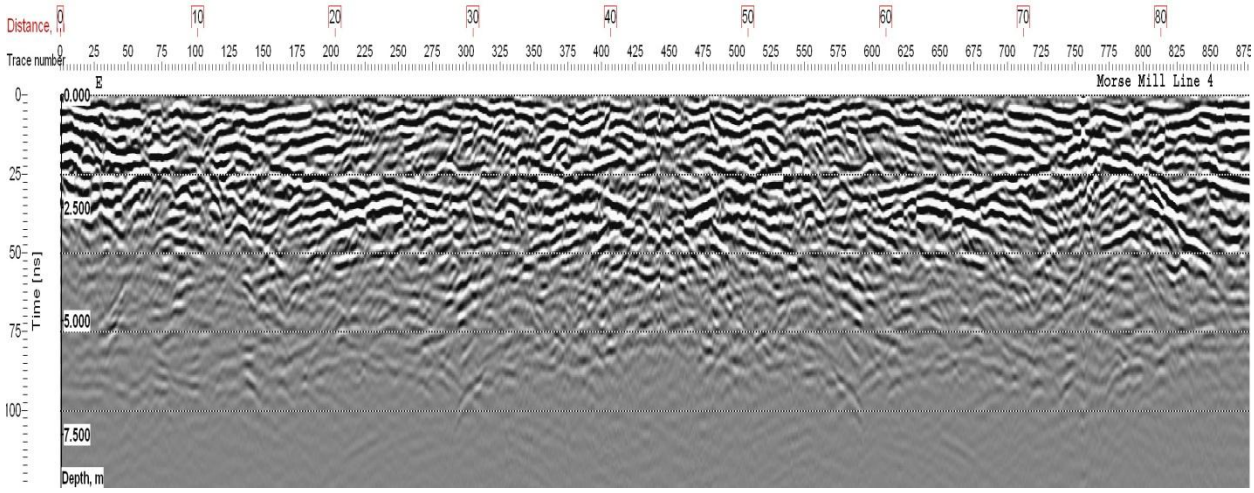

Figure 32. Processed 250 MHz GPR profile along line 4 parallel to the Big River across the gravel bar at Morse Mill.

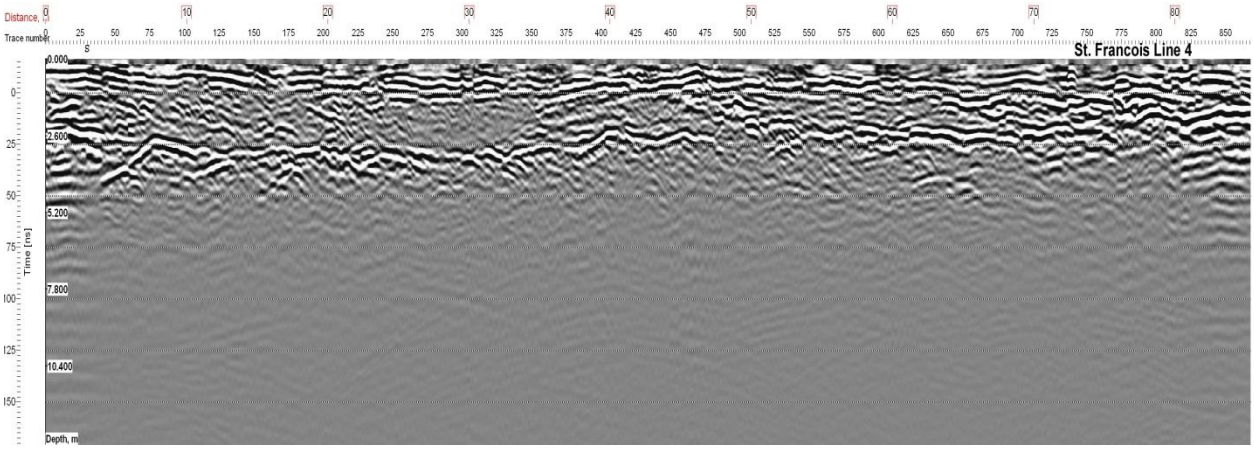

Figure 33. Processed 250 MHz GPR profile along line 4 perpendicular to the Big River across the gravel bar at St. Francois State Park.

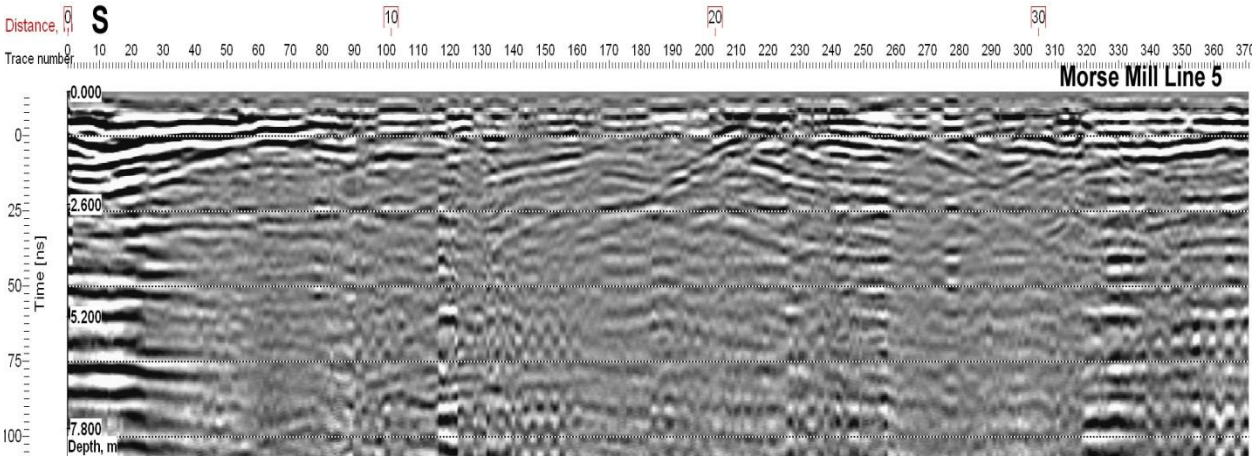

Figure 34. Processed 250 MHz GPR profile along line 5 perpendicular to the Big River across the gravel bar at Morse Mill.

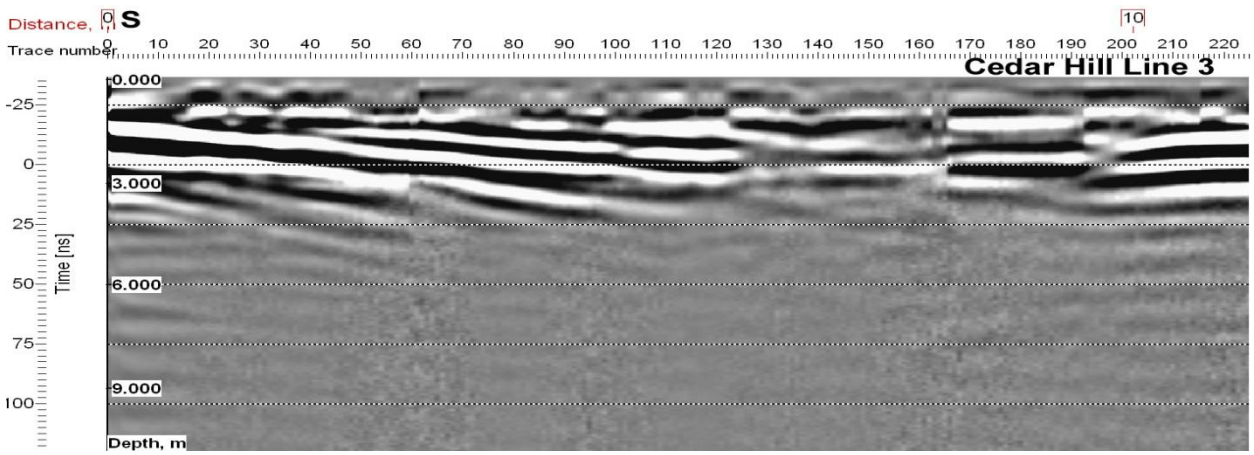

Figure 35. Processed 250 MHz GPR profile along line 3 perpendicular to the Big River across the gravel bar at Cedar Hill.